AIMS Mathematics, 10(12): 28151–28181.
DOI: 10.3934/math.20251238
Received: 20 July 2025
Revised: 17 October 2025
Accepted: 11 November 2025
Published: 01 December 2025

https://www.aimspress.com/journal/Math

Research article

Accelerated Hager-Zhang type projection scheme for monotone equations with applications

Abubakar Sani Halilu[1,2,3,4], Mohamad A. Mohamed[1], Mohammed A. Saleh[5], Kabiru Ahmed[1,2], Abdulgader Z. Almaymuni[5,*], Mohammed Y. Waziri[1,2], Sulaiman M. Ibrahim[6,7] and Badr Almutairi[8]

[1] Faculty of Informatics and Computing, Universiti Sultan Zainal Abidin, Besut, Malaysia
[2] Numerical Optimization Research Group, Bayero University, Kano, Nigeria
[3] Mathematics Department, Sule Lamido University (SLU) Kafin Hausa, Nigeria
[4] Mathematical Innovation and Applications Research Group, SLU, Kafin Hausa, Nigeria
[5] Department of Cybersecurity, College of Computer, Qassim University, Saudi Arabia
[6] School of Quantitative Science, Universiti Utara Malaysia, Sintok, Malaysia
[7] Faculty of Education and Arts Sohar University, Sohar 311, Oman
[8] College of Computer and Information Sciences, Majmaah University, Almajmaah , Saudi Arabia

* **Correspondence:** Email: almaymuni@qu.edu.sa.

Abstract: This paper proposed a new iterative method for solving nonlinear monotone equations with convex constraint and its applications in sparse signal reconstruction and image de-blurring problems. The method can be viewed as an improved adaptation of the generalized Hager-Zhang conjugate gradient method for unconstrained optimization. Unlike the latter which only converged globally for strongly convex functions when the Hager-Zhang parameter θ_k lies in the interval $\left(\frac{1}{4}, +\infty\right)$, the new method exhibited this attribute for nonlinear monotone and Lipschitz continuous functions without restriction for θ_k under a more relaxed condition. The derivative-free structure of the method made it suitable for both smooth and non-smooth problems. Numerical experiments on benchmark test problems demonstrated the method's superior performance compared to some state-of-the-art algorithms. Furthermore, the algorithm was successfully applied to sparse signal recovery and image de-blurring problems in compressed sensing, confirming its practical effectiveness.

Keywords: nonlinear monotone equations; convex constraint; conjugate gradient method; sparse signal reconstruction; image de-blurring; image reconstruction; optimization method
Mathematics Subject Classification: 90C26, 90C30

1. Introduction

System of nonlinear monotone equations is a concept that researchers have paid much interest in over the past decades. This is mostly due to its importance in real life applications. The general form of the concept is formulated as

$$F(\bar{a}) = 0, \ \ \bar{a} \in \mathbb{R}^n, \tag{1.1}$$

with the vector-valued mapping F assumed to be continuous and monotone. The monotonicity assumption means F satisfies

$$(F(a) - F(b))^T(a - b) \geq 0, \ \ \forall a, b \in \mathbb{R}^n. \tag{1.2}$$

In this paper, the solution of (1.1) $\bar{a}$ resides within a nonempty closed convex set $\mathcal{B} \subseteq \mathbb{R}^n$. This constrained form frequently appears in real-life problems such as economic and chemical equilibrium systems in [1, 2]. It is also essential in compressed sensing [3–5].

The most preferred iterative schemes designed to handle (1.1) and the variant described above, are the Newton's scheme and its improved variant, the quasi-Newton method [6, 7], due to their fast convergence attribute, especially when the initial guess is in a neighborhood of the solution. These methods are, however, computationally expensive to implement since they require obtaining the Jacobian or its approximation and their inverses at every iteration. The projection method designed in [8] by Solodov and Svaiter, by virtue of its global convergence attribute, and adaptations of the conjugate gradient (CG) schemes for large-scale problems, which require low memory to implement, have been combined to solve (1.1) and its constrained version. In [9], Cheng combined a modified Polak-Ribi'ere-Polyak (PRP) CG method [10, 11] with the hyperplane scheme [8] and proposed an effective algorithm to solve (1.1). Without differentiability requirement, and by employing basic conditions, the method is proven to converge globally. An improved variant of the PRP method [10, 11] was later developed by Yu in [12], where it is implemented with the strategy developed by Grippo et al. and Li and Fukushima [13, 14]. Based on a modified version of the Dai-Liao (DL) CG method [15], Halilu et al. [16] proposed a DL-type algorithm for the constrained version of (1.1) with its application to motion control. In an attempt to improve numerical efficiency of CG-type methods, Jiang and Huang [17] proposed a CG projection scheme with a restart strategy for constrained nonlinear monotone equations. The authors proved global convergence of the method and applied it to image de-blurring problems. By employing an adaptive CG and quasi-Newton search directions, as well as the strategy used in [18], Salihu et al. [19] proposed a spectral CG projection method for solving monotone nonlinear equations with signal processing application. The authors proved global convergence of the scheme under mild conditions. Based on a three-term search direction and an inertial strategy, Yin et al. [20] also proposed a CG projection method for solving constrained form of (1.1) with some real-life applications. In a recent development, Ahmed et al. [21] proposed a four-term adaptation of the DL method for solving the constrained form of (1.1). The authors proved global convergence of the scheme under some mild assumptions.

In the last decade, the Hager-Zhang (HZ) CG technique [22, 23] has been adopted to address the problem outlined in Eq (1.1) and its constrained variant. Typically, search direction of the HZ method is defined as

$$d_k = -F_k + \beta_k^{HZ} d_{k-1}, \ \ F_k = F(a_k), \ \ k = 1, 2, ..., \tag{1.3}$$

where

$$\beta_k^{HZ} = \frac{F_k^T y_{k-1}}{d_{k-1}^T y_{k-1}} - \theta_k \frac{\|y_{k-1}\|^2 F_k^T d_{k-1}}{(d_{k-1}^T y_{k-1})^2}, \tag{1.4}$$

with θ_k being a nonnegative parameter, $y_{k-1} = F_k - F_{k-1}$, and $F_{k-1} = F(a_{k-1})$. To apply the HZ method to solve (1.1) and its constrained variant, researchers derive appropriate values for θ_k in (1.4) and combine the search direction (1.3) with the projection approach developed in [8]. For example, Xiao and Zhu introduced a modified HZ-type projection method to solve (1.1) with convex constraints in their work [4] by employing (1.3), where θ_k in (1.4) is chosen to be 2. The algorithm obtained exhibits global convergence and is particularly relevant in the context of compressed sensing. In the same vein, Liu and Li [3] combined a modified version of the search direction presented in [4] with the technique described in [8] to present another HZ-type scheme for solving (1.1) with convex constraints. A key feature of this system, which makes it suitable for handling non-smooth functions, is its derivative-free and low-memory architecture. The authors have successfully applied this approach in compressive sensing to recover corrupted data.

By deriving two effective choices for the HZ parameter θ_k in (1.4), Waziri et al. [24] combined a modified version of the search direction (1.3) with the projection method [8] to propose a family of HZ-type methods for solving (1.1). The authors proved global convergence of the methods by applying some mild assumptions. Building on the work in [24], Sabi'u et al. [25] provided two new estimates for the HZ parameter in [23], leading to the creation of further HZ-type methods. Inspired by [25], Waziri et al. [26] further proposed two additional HZ-type methods for solving the constrained version of (1.1) with compressed sensing applications.

As presented in (1.4) and in the classical HZ update [23], the parameter θ_k is nonnegative, namely, it lies in the interval $[0, +\infty)$. However, the sufficient descent condition necessary for global convergence of the method only holds for $\theta_k \in (\frac{1}{4}, +\infty)$. This is true for all the HZ-type schemes discussed above. In an attempt to further study the HZ scheme, Ahmed et. al [27] proposed two HZ-type methods with strict conditions that ensure convergence when θ_k is in the interval $(0, \frac{1}{4})$. Recently, Ahmed et al. [28] proposed a double parameter HZ-type method for solving the constrained form of (1.1). The authors obtained an appropriate value for the HZ parameter θ_k that ensured clustering of the scheme's search direction matrix. The method converged globally and was applied to solve signal and image recovery problems. As a contribution, by relaxing one of the conditions applied in [27], a numerically efficient HZ-type projection scheme is proposed in this paper for the constrained form of (1.1), where the HZ parameter lies in the interval $(0, +\infty)$. The scheme's efficiency is further demonstrated by applying it to solve problems in compressed sensing.

The article is structured as follows: Section 2 outlines some preliminary steps necessary for generating the new scheme. Algorithm of the proposed method and its global convergence are presented in Section 3. The numerical results of the scheme are reported in Section 4. Section 5 explains how the proposed method is applied to compressive sensing problems, demonstrating its efficacy. Finally, Section 6 provides concluding remarks.

2. Preliminaries

Here, we first recall the popular unconstrained optimization problem defined by

$$\min_{a \in \mathbb{R}^n} f(a), \tag{2.1}$$

where f in (2.1) denotes a nonlinear function whose gradient $\nabla f(a_k) = g(a_k)$ is obtainable.

Various iterative schemes for solving (2.1) with double parameters have been developed in the literature. For example, modifications have been made to the popular quasi-Newton update by Broyden [29], Fletcher [30], Goldfarb [31], and Shanno [32], the (BFGS) scheme, specifically,

$$B_k = B_{k-1} - \frac{B_{k-1}s_{k-1}s_{k-1}^T B_{k-1}}{s_{k-1}^T B_{k-1}s_{k-1}} + \frac{y_{k-1}y_{k-1}^T}{s_{k-1}^T y_{k-1}}, \tag{2.2}$$

where B_k is a symmetric matrix, $s_{k-1} = a_k - a_{k-1}$, and $y_{k-1} = g(a_k) - g(a_{k-1})$.

Liao [33], proposed a two parameter modified BFGS scheme with update given by

$$B_k = B_{k-1} - \overline{\sigma}_k \frac{B_{k-1}s_{k-1}s_{k-1}^T B_{k-1}}{s_{k-1}^T B_{k-1}s_{k-1}} + \overline{\gamma}_k \frac{y_{k-1}y_{k-1}^T}{s_{k-1}^T y_{k-1}}. \tag{2.3}$$

The parameters $\overline{\sigma}_k$ and $\overline{\gamma}_k$ are introduced in the second and final terms of (2.2) to enhance the correction of the eigenvalues of the direction matrix used in the method. Numerical experiments involving over 80 benchmark test problems of various structures and complexities demonstrated a significant improvement of (2.3) compared to the classical BFGS scheme. Additionally, Andrei [34] proposed a double parameter BFGS scheme, with the update for the approximation of the Hessian matrix specified by

$$B_k = \overline{\sigma}_k \left[B_{k-1} - \frac{B_{k-1}s_{k-1}s_{k-1}^T B_{k-1}}{s_{k-1}^T B_{k-1}s_{k-1}} \right] + \overline{\gamma}_k \frac{y_{k-1}y_{k-1}^T}{s_{k-1}^T y_{k-1}}. \tag{2.4}$$

In (2.4) above, $\overline{\sigma}_k$ and $\overline{\gamma}_k$ represent positive parameters. Recently, Babaie-Kafaki [35] introduced a two-parameter BFGS scheme, which serves as an extension of the one proposed in [33]. The update of the scheme is given by

$$H_k = \overline{\tau}_k I - \overline{\tau}_k \frac{s_{k-1}y_{k-1}^T + y_{k-1}s_{k-1}^T}{s_{k-1}^T y_{k-1}} + \left(1 + \overline{\gamma}_k \frac{\|y_{k-1}\|^2}{s_{k-1}^T y_{k-1}}\right) \frac{s_{k-1}s_{k-1}^T}{s_{k-1}^T y_{k-1}}, \tag{2.5}$$

where, $\overline{\tau}_k$ and $\overline{\gamma}_k$ represent two positive parameters. The author established that the necessary condition for the global convergence of the method is fulfilled. Specifically,

$$g_k^T d_k \leq -\psi \|g_k\|^2, \quad \forall k \geq 0, \quad \psi > 0.$$

Furthermore, the author demonstrated that the condition number related to the search direction matrix of the scheme remains in a more favorable condition. A modified version of (2.5) was proposed in [36], namely,

$$H_k = \frac{1}{\overline{\delta}_k} \left[H_{k-1} - \frac{H_{k-1}y_{k-1}s_{k-1}^T + s_{k-1}y_{k-1}^T H_{k-1}}{s_{k-1}^T y_{k-1}} + \left(\frac{\overline{\delta}_k}{\overline{\gamma}_k} + \frac{y_{k-1}^T H_{k-1} y_{k-1}}{s_{k-1}^T y_{k-1}} \right) \frac{s_{k-1}s_{k-1}^T}{s_{k-1}^T y_{k-1}} \right], \tag{2.6}$$

where $\overline{\delta}_k$ and $\overline{\gamma}_k$ are parameters determined by employing Byrd and Nocedal's measure function in [37].

To enhance the numerical implementation of the classical one-parameter HZ scheme [23], Babaie-Kafaki [38] proposed a variant that scales the second and third terms in the search direction of the method, namely,

$$d_k = -g_k + \gamma \beta_k^{\theta} d_{k-1}, \tag{2.7}$$

where

$$\beta_k^{\theta} = \frac{g_k^T y_{k-1}}{d_{k-1}^T y_{k-1}} - \theta_k \frac{\|y_{k-1}\|^2 g_k^T d_{k-1}}{(d_{k-1}^T y_{k-1})^2}, \quad k \geq 1, \tag{2.8}$$

with $\gamma \in [0, 1]$. Based on (2.7) and (2.8), the direction of the scheme can be rewritten as follows:

$$d_k = -G_k g_k,$$

where

$$G_k = I - \frac{\gamma s_{k-1} y_{k-1}^T}{s_{k-1}^T y_{k-1}} + \frac{\gamma \theta_k \|y_{k-1}\|^2 s_{k-1} s_{k-1}^T}{(s_{k-1}^T y_{k-1})^2}.$$

It has been established in [38] that for values of θ_k satisfying the condition $\theta_k \geq \bar{\theta} > \frac{1}{4}$, the new HZ scheme presented in (2.7) fulfills the necessary criteria below

$$d_k^T g_k \leq -\left(1 - \frac{\gamma}{4\theta_k}\right)\|g_k\|^2, \quad \forall k \geq 1.$$

3. New modified HZ-type scheme

In the first section, it was highlighted that several modified HZ-type schemes are available for addressing problem (1.1) as well as its constrained variant. Also, each scheme involves a different approximation of the HZ parameter θ_k, which has been shown to satisfy the inequality

$$d_k^T F_k \leq -\psi \|F_k\|^2, \tag{3.1}$$

with

$$\psi = \left(1 - \frac{1}{4\theta_k}\right), \quad \theta_k \geq \bar{\theta} > \frac{1}{4}.$$

These include the schemes proposed by Waziri et al. [24], where the authors obtained the following values of θ_k

$$\theta_{k1} = \xi - \psi \frac{(s_{k-1}^T y_{k-1})^2}{\|y_{k-1}\|^2 \|s_{k-1}\|^2}, \quad \theta_{k2} = \xi - \psi \frac{(s_{k-1}^T z_{k-1})^2}{\|z_{k-1}\|^2 \|s_{k-1}\|^2}, \quad \xi > \frac{1}{4}, \psi \leq 0,$$

where

$$z_{k-1} = y_{k-1} + \zeta \frac{\max\{\hat{\vartheta}_{k-1}, 0\}}{s_{k-1}^T d_{k-1}} d_{k-1}, \quad \hat{\vartheta}_{k-1} = 6(f_{k-1} - f_k) + 3 s_{k-1}^T (F_{k-1} + F_k), \quad \zeta > 0. \tag{3.2}$$

The authors have shown that both algorithms converged globally for the given values of θ_k, which are clearly greater than $\frac{1}{4}$. Also, Sabi'u et al. [39] presented two HZ-type approaches and their parameters choices are given as

$$\theta_{k1}^* = \frac{(s_{k-1}^T \hat{y}_{k-1})^2}{\|s_{k-1}\|^2 \|\hat{y}_{k-1}\|^2}, \quad \theta_{k2}^* = \sqrt{\frac{\|s_{k-1}\| \|\hat{y}_{k-1}\|}{s_{k-1}^T \hat{y}_{k-1}}},$$

where

$$\hat{y}_{k-1} = y_{k-1} + \rho \frac{\max\{\hat{\vartheta}_{k-1}, 0\}}{s_{k-1}^T s_{k-1}} s_{k-1}, \quad \rho \in [0, 1], \tag{3.3}$$

with $\hat{\vartheta}_{k-1}$ as defined in (3.2). The authors in [39] also presented adaptive versions of the HZ CG method in [25] for (1.1) with convex constraint with new choices for the parameter θ_k, namely,

$$\theta^*_{k3} = 1 + \sqrt{1 + \left(\frac{s^T_{k-1}\hat{y}_{k-1}}{\|s_{k-1}\|\|\hat{y}_{k-1}\|}\right)^2},$$

and

$$\theta^*_{k4} = \frac{\|s_{k-1}\|^2\|\hat{y}_{k-1}\|^2}{(s^T_{k-1}\hat{y}_{k-1})^2} + \sqrt{\frac{(s^T_{k-1}\hat{y}_{k-1})^2}{\|s_{k-1}\|^2\|\hat{y}_{k-1}\|^2} + \frac{\|s_{k-1}\|^4\|\hat{y}_{k-1}\|^4}{(s^T_{k-1}\hat{y}_{k-1})^4}},$$

where $\hat{y}_{k-1}$ is as defined by (3.3) and $\hat{\vartheta}_{k-1}$ as defined in (3.2). Only recently, Sabi'u et al. [40] developed two additional adaptive versions of the HZ schemes with their parameters defined as

$$\theta^*_{k5} = \frac{(s^T_{k-1}\hat{y}_{k-1})^2}{\|s_{k-1}\|^2\|\hat{y}_{k-1}\|^2} + \frac{s^T_{k-1}\hat{y}_{k-1}}{\|s_{k-1}\|\|\hat{y}_{k-1}\|}, \quad \theta^*_{k6} = \frac{s^T_{k-1}\hat{y}_{k-1}}{\|s_{k-1}\|\|\hat{y}_{k-1}\|},$$

where $\hat{y}_{k-1}$ and $\hat{\vartheta}_{k-1}$ remain as defined in (3.3) and (3.2), respectively. As a result, the authors demonstrate that the schemes converge globally in all illustrations explained above and satisfy the inequality (3.1) for $\theta_k = \bar{\theta} \in (\frac{1}{4}, +\infty)$. Recently, Ahmed et. al [27] proposed the following HZ-type search direction:

$$d_k = -F_k + \beta_k s_{k-1}, \quad F_k = F(a_k), \quad k = 1, 2, ...,$$

where

$$\beta_k = \frac{F^T_k \bar{y}_{k-1}}{s^T_{k-1}\bar{y}_{k-1}} - \gamma\theta_k \frac{\|\bar{y}_{k-1}\|^2 F^T_k s_{k-1}}{(s^T_{k-1}\bar{y}_{k-1})^2}, \gamma > 1,$$

and

$$\bar{y}_{k-1} = \tilde{y}_{k-1} + \phi_{k-1}s_{k-1}, \quad \phi_{k-1} = 1 + \max\left\{0, -\frac{s^T_{k-1}\tilde{y}_{k-1}}{\|s_{k-1}\|^2}\right\}, \quad \tilde{y}_{k-1} = y_{k-1} + c\frac{F^T_k s_{k-1}}{\|s_{k-1}\|}s_{k-1},$$

with $c > 0$ and $s_{k-1} = a_k - a_{k-1}$. The authors proved that the scheme converges globally under the monotonicity and strong Lipschitz assumptions when $\theta_k = \bar{\theta} > \frac{1}{4\gamma}$ and $\gamma > 1$. Under these two conditions, the inequality (3.1) holds for $\theta_k = \bar{\theta} \in (0, +\infty)$. Moreover, the authors obtained the following choices of the parameter θ_k for which the aforemention condition holds.

$$\bar{\theta}_{k1} = \max\{\theta^*_{k1}, \varepsilon_1\}, \quad \varepsilon_1 = \frac{\tilde{z}}{4\gamma}, \quad \tilde{z} \in \mathbb{Z}^+ > 1.$$

and

$$\bar{\theta}_{k2} = \max\{\theta^*_{k2}, \varepsilon_2\}, \quad \varepsilon_2 = \frac{\bar{z}}{4\gamma}, \quad \bar{z} \in \mathbb{Z}^+ > 1.$$

In light of the discussion presented in Section 2 and influenced by (2.5), (2.6), and the work in [27], we proceed to derive a new version of the HZ scheme and prove it converges globally and satisfies the inequality (3.1) for $\theta_k = \bar{\theta} \in (0, +\infty)$ under the condition that $\gamma \in (\frac{1}{4}, 2)$. The scheme's search direction is given by

$$d_k = -\theta_k F_k + \frac{\theta_k F^T_k \bar{y}_{k-1}}{s^T_{k-1}\bar{y}_{k-1}}s_{k-1} - \gamma\theta_k \frac{\|\bar{y}_{k-1}\|^2 F^T_k s_{k-1}}{(s^T_{k-1}\bar{y}_{k-1})^2}s_{k-1}, \quad d_0 = -F_0, \tag{3.4}$$

where

$$\bar{y}_{k-1} = y_{k-1} + \varsigma s_{k-1}, \;\; y_{k-1} = F(\vartheta_{k-1}) - F(a_{k-1}), \;\; \vartheta_{k-1} = a_{k-1} + \sigma_{k-1} d_{k-1}, \;\; \varsigma > 0, \tag{3.5}$$

and $s_{k-1} = \vartheta_{k-1} - a_{k-1}$.

From (3.5), and by monotonicity of F, we have

$$s_{k-1}^T \bar{y}_{k-1} = s_{k-1}^T y_{k-1} + \varsigma \|s_{k-1}\|^2 \geq \varsigma \|s_{k-1}\|^2 > 0, \;\; \varsigma > 0. \tag{3.6}$$

Hence, (3.4) is well-defined.

Lemma 3.1. *The sequence* $\{d_k\}$ *defined by* (3.4) *satisfies the inequality*

$$d_k^T F_k \leq -\psi \|F_k\|^2, \;\; \theta_k = \bar{\theta} \in (0, \infty), \;\; k \geq 1, \tag{3.7}$$

where $\psi = \bar{\theta}\left(1 - \frac{1}{4\gamma}\right), \gamma \in \left(\frac{1}{4}, 2\right)$.

Proof. It is interesting that the search direction in (3.4) can be rewritten as

$$d_k = -M_k F_k, \quad \forall k \geq 1,$$

where M_k is the scheme's iteration matrix, which means

$$M_k = \theta_k I - \frac{\theta_k s_{k-1} \bar{y}_{k-1}^T}{s_{k-1}^T \bar{y}_{k-1}} + \frac{\gamma \theta_k \|\bar{y}_{k-1}\|^2 s_{k-1} s_{k-1}^T}{(s_{k-1}^T \bar{y}_{k-1})^2}. \tag{3.8}$$

It is clear that the matrix M_k is not symmetric and not positive definite. We can get a symmetric version of (3.8) by

$$\overline{M}_k = \frac{1}{2}[M_k^T + M_k],$$

or more precisely, as

$$\overline{M}_k = \theta_k I - \frac{\theta_k s_{k-1} \bar{y}_{k-1}^T}{2 s_{k-1}^T \bar{y}_{k-1}} - \frac{\theta_k \bar{y}_{k-1} s_{k-1}^T}{2 s_{k-1}^T \bar{y}_{k-1}} + \frac{\gamma \theta_k \|\bar{y}_{k-1}\|^2 s_{k-1} s_{k-1}^T}{(s_{k-1}^T \bar{y}_{k-1})^2}. \tag{3.9}$$

So, in compact form, the revised search direction becomes

$$d_k = -\overline{M}_k F_k, \quad \forall k \geq 1. \tag{3.10}$$

Now, considering (3.10), we can write

$$d_k^T F_k = -F_k^T \overline{M}_k F_k, \quad \forall k \geq 1. \tag{3.11}$$

Next, we analyze eigenvalues of the matrix $\overline{M}_k$ and their structure. Since from (3.6) $s_{k-1}^T \bar{y}_{k-1} > 0$, hence, $s_{k-1} \neq 0$ and $\bar{y}_{k-1} \neq 0$. Now let's look at two possibilities:

(i). $s_{k-1} \nparallel \bar{y}_{k-1}$. This indicates the existence of a set of vectors, say $\{\upsilon_{k-1}^i\}_{i=1}^{n-2} \subset \mathcal{S}^{\perp}$ for which

$$s_{k-1}^T \upsilon_{k-1}^i = \bar{y}_{k-1}^T \upsilon_{k-1}^i = 0, \;\; i = 1, ..., n-2, \tag{3.12}$$

where $\mathcal{S}^{\perp}$ denotes the orthogonal complement of the space $\mathcal{S} \subset \mathbb{R}^n$ spanned by the vectors s_{k-1} and $\bar{y}_{k-1}$. In addition to (3.12), we get

$$\overline{M}_k \upsilon_{k-1}^i = \overline{M}_k^T \upsilon_{k-1}^i = \theta_k \upsilon_{k-1}^i, \quad i = 1, ..., n-2,$$

which implies that for $i = 1, ..., n-2$, the vectors υ_{k-1} are eigenvectors of $\overline{M}_k$ corresponding to the eigenvalue θ_k. We then look for the two remaining eigenvalues of $\overline{M}_k$, which we label as χ_k^+ and χ_k^-.

Now, from (3.9), trace of $\overline{M}_k$ can be obtained as

$$\begin{aligned} \mathrm{tr}(\overline{M}_k) &= n\theta_k - \theta_k + \frac{\gamma\theta_k \|\bar{y}_{k-1}\|^2 \|s_{k-1}\|^2}{(s_{k-1}^T \bar{y}_{k-1})^2} \\ &= \underbrace{\theta_k + ... + \theta_k}_{\text{(n-2) times}} + \chi_k^+ + \chi_k^-, \end{aligned}$$

which ultimately yields

$$\chi_k^+ + \chi_k^- = \theta_k + \frac{\gamma\theta_k \|\bar{y}_{k-1}\|^2 \|s_{k-1}\|^2}{(s_{k-1}^T \bar{y}_{k-1})^2}. \tag{3.13}$$

Additionally, by applying the Frobenius norm's properties and setting $\Lambda_k = \frac{\|\bar{y}_{k-1}\| \|s_{k-1}\|}{(s_{k-1}^T \bar{y}_{k-1})}$, we have

$$\begin{aligned} \|\overline{M}_k\|_F^2 &= \mathrm{tr}(\overline{M}_k^T \overline{M}_k) \\ &= n\theta_k^2 - \frac{3}{2}\theta_k^2 + \frac{\theta^2 \Lambda_k^2}{2} + \gamma^2 \theta_k^2 \Lambda_k^4 \\ &= \underbrace{\theta_k^2 + ... + \theta_k^2}_{\text{(n-2) times}} + \chi_k^{+2} + \chi_k^{-2}, \end{aligned}$$

which subsequently yields

$$\chi_k^{+2} + \chi_k^{-2} = \frac{\theta_k^2}{2} + \frac{\theta_k^2 \Lambda_k^2}{2} + \gamma^2 \theta_k^2 \Lambda_k^4. \tag{3.14}$$

Also, from (3.13) and (3.14), we get

$$\chi_k^- \chi_k^+ = \frac{\theta_k^2}{4} + \gamma\theta_k^2 \Lambda_k^2 - \frac{\theta_k^2 \Lambda_k^2}{4}. \tag{3.15}$$

Now, from (3.13) and (3.15), we deduce that χ_k^+ and χ_k^- are just solutions to the polynomial equation

$$\chi^2 - \left(\theta_k + \gamma\theta_k \Lambda_k^2\right)\chi + \frac{\theta_k^2}{4} + \gamma\theta_k^2 \Lambda_k^2 - \frac{\theta_k^2 \Lambda_k^2}{4} = 0,$$

which can be obtained in more precise form as

$$\chi_k^{\pm} = \frac{1}{2}\left[\theta_k + \gamma\theta_k \Lambda_k^2 \pm \sqrt{\gamma^2 \theta_k^2 \Lambda_k^4 + (1-2\gamma)\theta_k^2 \Lambda_k^2}\right],$$

or by following some simplification as

$$\chi_k^{\pm} = \frac{1}{2}\left[\theta_k + \gamma\theta_k \Lambda_k^2 \pm \sqrt{(\theta_k \Lambda_k - \theta_k \gamma \Lambda_k)^2 + \theta_k^2 \gamma^2 \Lambda_k^4 - \theta_k^2 \gamma^2 \Lambda_k^2}\right]. \tag{3.16}$$

From (3.16) and the Cauchy Schwarz inequality, it is clear that $\chi_k^+ > 0$. Also, to establish that $\chi_k^- > 0$, the following function can be defined:

$$G(\eta) = \frac{1}{2}\left[\theta_k + \gamma\theta_k\eta^2 - \eta\theta_k\sqrt{\gamma^2\eta^2 + (1-2\gamma)}\right].$$

Now, it is worth noting that $G(\Lambda_k) = \chi_k^-$ and $G(\eta)$ is a strictly decreasing function on $[1, +\infty)$ for $\theta_k \in (0, +\infty)$ and $\gamma \neq \frac{1}{2}$. Additionally, since $\gamma \in (\frac{1}{4}, 2)$, taking limits as η approaches infinity of $G(\eta)$ yields

$$\chi_k^- > \lim_{\eta\to\infty} G(\eta) = \theta_k - \frac{\theta_k}{4\gamma} = \theta_k\left(1 - \frac{1}{4\gamma}\right) > 0.$$

Moreover, if $\gamma = \frac{1}{2}$, we have

$$\chi_k^- = \frac{\theta_k}{2} = \theta_k - \frac{\theta_k}{2} = \theta_k\left(1 - \frac{1}{4\gamma}\right) > 0.$$

(ii). $s_{k-1} \parallel \bar{y}_{k-1}$. According to this possibility, there exists a nonzero constant τ for which $\bar{y}_{k-1} = \tau s_{k-1}$. Applying this in (3.8) or (3.9) leads to

$$M_k = \overline{M}_k = \theta_k I - \frac{\theta_k s_{k-1}s_{k-1}^T}{\|s_{k-1}\|^2} + \frac{\gamma\theta_k s_{k-1}s_{k-1}^T}{\|s_{k-1}\|^2}.$$

Since $s_{k-1} \neq 0$, as previously mentioned, there is a set of mutually orthogonal vectors $\{\upsilon_{k-1}^i\}_{i=1}^{n-1} \subset \mathcal{S}^\perp$ for which

$$s_{k-1}^T\upsilon_{k-1}^i = 0, \;\; \|\upsilon_{k-1}^i\| = 1, \;\; i = 1, ..., n-1,$$

which consequently leads to

$$\overline{M}_k\upsilon_{k-1}^i = \theta_k\upsilon_{k-1}^i, \quad i = 1, ..., n-1.$$

This indicates that the eigenvalue of $\overline{M}_k$ is θ_k, with a multiplicity of $n-1$. The set of eigenvectors associated with $\overline{M}_k$ is represented by $\{\upsilon_{k-1}^i\}_{i=1}^{n-1}$. Furthermore,

$$\overline{M}_k s_{k-1} = \theta_k s_{k-1} - \frac{\theta_k s_{k-1}s_{k-1}^T}{\|s_{k-1}\|^2}s_{k-1} + \frac{\gamma\theta_k s_{k-1}s_{k-1}^T}{\|s_{k-1}\|^2}s_{k-1} = (\gamma\theta_k)s_{k-1},$$

which also indicates that s_{k-1} is the eigenvector of $\overline{M}_k$, and $\bar{\chi}_k$ is the corresponding eigenvalue, namely,

$$\bar{\chi}_k = \gamma\theta_k.$$

Given that $\theta_k > 0$ and $\gamma \in (\frac{1}{4}, 2)$ are parameters, it can be demonstrated that

$$\bar{\chi}_k = \theta_k\gamma > \theta_k\left(1 - \frac{1}{4\gamma}\right) > 0, \;\; \forall k.$$

Additionally, if χ_s is the least eigenvalue of $\overline{M}_k$, then using the two options previously examined, we can get

$$\chi_s \geq \theta_k\left(1 - \frac{1}{4\gamma}\right) > 0.$$

Consequently, the aforementioned analysis demonstrates that $\overline{M}_k$ is positive-definite. Therefore, utilizing (3.11), and for $\theta_k = \bar{\theta} \in (0, +\infty)$, we get

$$d_k^T F_k = -F_k^T \overline{M}_k F_k \leq -\chi_s \|F_k\|^2 \leq -\bar{\theta}\left(1 - \frac{1}{4\gamma}\right)\|F_k\|^2.$$

On the other hand, if we set $\Delta_k = s_{k-1}^T \bar{y}_{k-1}$, then by direct calculation, we have

$$\begin{aligned} d_k^T F_k &= -\theta_k \|F_k\|^2 + \frac{\theta_k F_k^T \bar{y}_{k-1}}{\Delta_k} F_k^T s_{k-1} - \gamma\theta_k \frac{\|\bar{y}_{k-1}\|^2 (F_k^T s_{k-1})^2}{\Delta_k^2} \\ &= \frac{\theta_k F_k^T \bar{y}_{k-1} \Delta_k F_k^T s_{k-1} - \theta_k \Delta_k^2 \|F_k\|^2 - \gamma\theta_k \|\bar{y}_{k-1}\|^2 (F_k^T s_{k-1})^2}{\Delta_k^2}. \end{aligned}$$

By setting $\nu_1 = \frac{\Delta_k \sqrt{\theta_k} F_k}{\sqrt{2\gamma}}$, $\nu_2 = \sqrt{2\gamma\theta_k}(F_k^T s_{k-1})\bar{y}_{k-1}$ and using the identity

$$\nu_1^T \nu_2 \leq \frac{1}{2}(\|\nu_1\|^2 + \|\nu_2\|^2),$$

we obtain

$$\begin{aligned} d_k^T F_k &\leq \frac{\frac{\theta_k \Delta_k^2 \|F_k\|^2}{4\gamma} + \gamma\theta_k \|\bar{y}_{k-1}\|^2 (F_k^T s_{k-1})^2 - \theta_k \Delta_k^2 \|F_k\|^2 - \gamma\theta_k \|\bar{y}_{k-1}\|^2 (F_k^T s_{k-1})^2}{\Delta_k^2} \\ &= -\theta_k \|F_k\|^2 + \frac{\theta_k}{4\gamma}\|F_k\|^2 \\ &= -\theta_k \left(1 - \frac{1}{4\gamma}\right)\|F_k\|^2. \end{aligned}$$

Therefore, if $\theta_k = \bar{\theta} \in (0, +\infty)$ for each $k \geq 1$ with $\gamma \in (\frac{1}{4}, 2)$, the proposed method satisfies (3.1). Hence, letting $\psi = \bar{\theta}_k \left(1 - \frac{1}{4\gamma}\right)$, we have

$$d_k^T F_k \leq \psi \|F_k\|^2, \tag{3.17}$$

which completes the proof. □

Following earlier research in [24,25,39], we go on to determine the proper value for the parameter θ_k of the modified HZ scheme. In order to do this, we employ the concept for analyzing the convergence of quasi-Newton schemes that Byrd and Nocedal [41] developed. The authors in [41] suggested the following measure function defined on any positive definite matrix:

$$\Phi(H) = \text{tr}(H) - \ln(\det(H)),$$

where, H denotes a positive-definite matrix with exclusively positive real eigenvalues, namely, $\chi_1 \geq \chi_2 \geq \ldots \geq \chi_n > 0$. Additionally, $\text{tr}(H)$ signifies the trace of H, while $\ln(\det(H))$ indicates the natural logarithm of the determinant of the matrix H. The authors observed that the function $\Phi(H)$ quantifies the proximity of H to an identity matrix, with $\Phi(I) = n$. Furthermore, the authors demonstrated that

the matrix H is ill-conditioned when $\Phi(H)$ is substantial. Consequently, the parameter θ_k may be determined as the minimizer of the function $\Phi(\overline{M}_k)$.

Using some algebraic simplifications from (3.13) and (3.15), we have

$$\theta_k = \arg\min_{\theta} \Phi(\overline{M}_k) = \frac{2(s_{k-1}^T \bar{y}_{k-1})^2}{(s_{k-1}^T \bar{y}_{k-1})^2 + \gamma \|\bar{y}_{k-1}\|^2 \|s_{k-1}\|^2}. \tag{3.18}$$

Prior to outlining the new scheme's algorithmic steps, we first go over the projection operator $P_{\mathcal{B}}[a]$, which is expressed as

$$P_{\mathcal{B}}[a] = \arg\min \|a - b\| : b \in \mathcal{B}, \quad \forall a \in \mathbb{R}^n.$$

Also, $P_{\mathcal{B}}[.]$ is nonexpansive, namely,

$$\|P_{\mathcal{B}}(a) - P_{\mathcal{B}}(b)\| \leq \|a - b\|, \quad \forall a, b \in \mathbb{R}^n,$$

and

$$\|P_{\mathcal{B}}(a) - b\| \leq \|a - b\|, \quad \forall b \in \mathcal{B}. \tag{3.19}$$

We now introduce the new scheme's algorithm as follows:

Algorithm 1 New Hager-Zhang Iterative Scheme (NHZIS)

Step 0: *Initialization*. Select an initial guess $a_0 \in \mathcal{B}$, tolerance $\varepsilon > 0$, parameters $\varsigma > 0$, $\gamma \in \left(\frac{1}{4}, 2\right)$, $\beta \in (0, 1)$, $\overline{\phi} \in (0, 2)$, $\rho \in (0, 1)$, $\mu > 0$. Set $k = 0$ and $d_0 = -F_0$.

Step 1: Calculate $F(a_k)$ and stop the process if $\|F(a_k)\| \leq \varepsilon$, otherwise, proceed to **Step** 2.

Step 2: Compute $\vartheta_k = a_k + \sigma_k d_k$, where $\sigma_k = \max\{\beta\rho^{\iota} : \iota = 0, 1, 2, ...\}$, such that

$$-F(\vartheta_k)^T d_k \geq \mu\sigma_k \|d_k\|^2, \tag{3.20}$$

is satisfied.

Step 3: If $\|F(\vartheta_k)\| \leq \epsilon$ stop, else set

$$a_{k+1} = P_{\mathcal{B}}\left[a_k - \overline{\phi}\varphi_k F(\vartheta_k)\right], \tag{3.21}$$

where

$$\varphi_k = \frac{F(\vartheta_k)^T (a_k - \vartheta_k)}{\|F(\vartheta_k)\|^2}. \tag{3.22}$$

Step 4: Generate direction d_{k+1} by (3.4) with θ_k given by (3.18).

Step 5: Set $k = k + 1$ and proceed to **Step** 1.

4. Analysis of the scheme's global convergence

In order to proceed with the analysis, we require the following assumptions:

(i). There exists $\bar{a} \in \mathcal{B}$ for which $F(\bar{a}) = 0$.

(ii). The mapping F is Lipschitz continuous, namely, for $0 < L < \infty$, the following is satisfied:

$$\|F(a) - F(b)\| \leq L\|a - b\|, \quad \forall a, b \in \mathbb{R}^n. \tag{4.1}$$

Lemma 4.1. *Suppose Assumption* (*i*) *holds. Then,* $\forall k \geq 0$*, there exists a positive constant* σ_k *such that* (3.20) *is satisfied.*

Proof. Assume, by contradiction, that there is a constant k_0 for which (3.20) does not hold for every integer $i \geq 0$, specifically,

$$-F(a_{k_0} + \beta\rho^i d_{k_0})^T d_{k_0} < \mu\beta\rho^i \|d_{k_0}\|^2.$$

Making use of Assumption (i) and allowing the integer i to increase to infinity, i.e., $i \to \infty$, results in

$$-F(a_{k_0})^T d_{k_0} \leq 0. \tag{4.2}$$

From (3.17), we obtain

$$-F(a_{k_0})^T d_{k_0} \geq \psi \|F(a_{k_0})\|^2 > 0. \tag{4.3}$$

A contradiction is obtained when taking into account (4.2) and (4.3), establishing the proof. □

Lemma 4.2. *Given that Assumptions* (*i*) *and* (*ii*) *hold, let* $\bar{a}$ *be an arbitrary solution of* (1.1) *in* $\mathcal{B}$*. Then the sequences* $\{a_k\}$ *and* $\{\vartheta_k\}$ *in Algorithm* 1 *are bounded and*

$$\lim_{k\to\infty} \|a_k - \vartheta_k\| = 0. \tag{4.4}$$

$$\lim_{k\to\infty} \|a_{k+1} - \vartheta_k\| = 0.$$

Proof. Now, we try to show that $\{a_k\}$ and $\{\vartheta_k\}$ are bounded. Suppose $\bar{a} \in \mathcal{B}$ denotes the solution of (1.1). From (1.2), we get

$$(a_k - \bar{a})^T F(\vartheta_k) \geq (a_k - \vartheta_k)^T F(\vartheta_k).$$

From (3.20) and definition of ϑ_k, we get

$$(a_k - \vartheta_k)^T F(\vartheta_k) \geq \mu\sigma_k^2 \|d_k\|^2. \tag{4.5}$$

Using (3.19) and (3.21), we obtain

$$\begin{aligned}
\|a_{k+1} - \bar{a}\|^2 &= \|P_{\mathcal{B}}(a_k - \overline{\phi}\varphi_k F(\vartheta_k)) - \bar{a}\|^2 \\
&\leq \|a_k - \overline{\phi}\varphi_k F(\vartheta_k) - \bar{a}\|^2 \\
&= \|a_k - \bar{a}\|^2 - 2\overline{\phi}\varphi_k F(\vartheta_k)^T(a_k - \bar{a}) + \overline{\phi}^2\varphi_k^2 \|F(\vartheta_k)\|^2 \\
&= \|a_k - \bar{a}\|^2 - 2\overline{\phi}\frac{F(\vartheta_k)^T(a_k - \vartheta_k)}{\|F(\vartheta_k)\|^2} F(\vartheta_k)^T(a_k - \bar{a}) + \overline{\phi}^2 \left(\frac{F(\vartheta_k)^T(a_k - \vartheta_k)}{\|F(\vartheta_k)\|}\right)^2 \\
&\leq \|a_k - \bar{a}\|^2 - 2\overline{\phi}\frac{F(\vartheta_k)^T(a_k - \vartheta_k)}{\|F(\vartheta_k)\|^2} F(\vartheta_k)^T(a_k - \vartheta_k) + \overline{\phi}^2 \left(\frac{F(\vartheta_k)^T(a_k - \vartheta_k)}{\|F(\vartheta_k)\|}\right)^2 \\
&= \|a_k - \bar{a}\|^2 - \overline{\phi}(2 - \overline{\phi}) \left(\frac{F(\vartheta_k)^T(a_k - \vartheta_k)}{\|F(\vartheta_k)\|}\right)^2 \\
&\leq \|a_k - \bar{a}\|^2,
\end{aligned} \tag{4.6}$$

which reduces to

$$\|a_{k+1} - \bar{a}\| \leq \|a_k - \bar{a}\|, \quad \forall k \geq 0. \tag{4.7}$$

Recursively, (4.7) indicates that $\|a_k - \bar{a}\| \leq \|a_0 - \bar{a}\|$, $\forall k$. Hence, $\{\|a_k - \bar{a}\|\}$ denotes a decreasing sequence, which is ultimately bounded. As a result, $\{a_k\}$ is also bounded. From Assumption (i), (4.1) and (4.7), we get

$$\|F(a_k)\| = \|F(a_k) - F(\bar{a})\| \leq L\|a_k - \bar{a}\| \leq L\|a_0 - \bar{a}\|.$$

This implies that the sequence $\{F(a_k)\}$ is bounded by letting $\overline{u} = L\|x_0 - \bar{a}\|$, namely,

$$\|F(a_k)\| \leq \overline{u}. \tag{4.8}$$

By definition of ϑ_k in step 2, (4.5), (1.2), and the Cauchy Schwarz inequality, we obtain

$$\mu\|a_k - \vartheta_k\| = \frac{\mu\|\sigma_k d_k\|^2}{\|a_k - \vartheta_k\|} \leq \frac{F(\vartheta_k)^T(a_k - \vartheta_k)}{\|a_k - \vartheta_k\|} \leq \frac{F(a_k)^T(a_k - \vartheta_k)}{\|a_k - \vartheta_k\|} \leq \|F(a_k)\|. \tag{4.9}$$

Also, from boundedness of $\{a_k\}$, (4.8) and (4.9), we see that $\{\vartheta_k\}$ is also bounded. Similarly, the boundedness of $\{\vartheta_k\}$, for any solution $\bar{a} \in \mathcal{B}$, implies that $\{\|\vartheta_k - \bar{a}\|\}$ is bounded, namely,

$$\|\vartheta_k - \bar{a}\| \leq \overline{v}, \;\; \overline{v} > 0.$$

Moreover, from (4.1), we get

$$\|F(\vartheta_k)\| = \|F(\vartheta_k) - F(\bar{a})\| \leq L\|\vartheta_k - \bar{a}\| \leq L\overline{v}. \tag{4.10}$$

Setting $\overline{w} = L\overline{v}$, we obtain boundedness of $\{F(\vartheta_k)\}$. Now, from (4.6), we have

$$\begin{aligned}\|a_{k+1} + \bar{a}\|^2 &\leq \|a_k + \bar{a}\|^2 - \overline{\phi}(2 - \overline{\phi})\frac{[F(\vartheta_k)^T(a_k - \vartheta_k)]^2}{\|F(\vartheta_k)\|^2} \\ &\leq \|a_k + \bar{a}\|^2 - \overline{\phi}(2 - \overline{\phi})\mu^2\frac{\|a_k - \vartheta_k\|^4}{\|F(\vartheta_k)\|^2},\end{aligned}$$

or

$$\overline{\phi}(2 - \overline{\phi})\|a_k - \vartheta_k\|^4 \leq \frac{\|F(\vartheta_k)\|^2}{\mu^2}(\|a_k - \bar{a}\|^2 - \|a_{k+1} - \bar{a}\|^2). \tag{4.11}$$

Furthermore, from (4.10) and (4.11) we obtain

$$\overline{\phi}(2 - \overline{\phi})\sum_{k=0}^{\infty}\|a_k - \vartheta_k\|^4 \leq \frac{\overline{w}^2}{\mu^2}\sum_{k=0}^{\infty}(\|a_k - \bar{a}\|^2 - \|a_{k+1} - \bar{a}\|^2) \leq \frac{\overline{w}^2}{\mu^2}\|a_0 - \bar{a}\|^2 < \infty. \tag{4.12}$$

Based on (4.12) and the convergent series property, we get

$$\lim_{k \to \infty}\|a_k - \vartheta_k\| = 0.$$

Then, by (3.19), (3.22) and the Cauchy Schwarz inequality, we get

$$\begin{aligned}\|a_{k+1} - a_k\| &= \|P_{\mathbb{B}}[a_k - \varphi_k F(\vartheta_k)] - a_k\| \\ &\leq \|a_k - \varphi_k F(\vartheta_k) - a_k\| \\ &= \|\varphi_k F(\vartheta_k)\| \\ &\leq \|a_k - \vartheta_k\|.\end{aligned} \tag{4.13}$$

Therefore, we obtain the following by taking the limit of both sides of (4.13):

$$\lim_{k\to\infty} \|a_{k+1} - a_k\| = 0.$$

Furthermore, from (4.4) and the knowledge that $\vartheta_k = \sigma_k d_k$, we get

$$\lim_{k\to\infty} \sigma_k \|d_k\| = 0. \tag{4.14}$$

□

Theorem 4.3. *Let Assumptions **(i)** and **(ii)** hold. Consider the sequences $\{a_k\}$ and $\{\vartheta_k\}$ generated by Algorithm* 1. *Then*

$$\liminf_{k\to\infty} \|F(a_k)\| = 0. \tag{4.15}$$

Proof. The proof is by contradiction. If (4.15) is not true, then there exists $v_1 > 0$ such that

$$\|F_k\| \geq v_1, \quad \forall k \geq 0. \tag{4.16}$$

Now, by the Cauchy Schwarz inequality and (3.7), we obtain that

$$\|d_k\| \geq \psi \|F_k\| \geq v_1, \quad \forall k \geq 0.$$

Also, by the Cauchy Schwarz inequality,

$$\frac{\|s_{k-1}\|^2 \|\bar{y}_{k-1}\|^2}{(s_{k-1}^T \bar{y}_{k-1})^2} \geq 1, \quad \forall k \geq 1,$$

which clearly implies that

$$\|s_{k-1}\|^2 \|\bar{y}_{k-1}\|^2 \geq (s_{k-1}^T \bar{y}_{k-1})^2,$$

and

$$\frac{1}{\|s_{k-1}\|^2 \|\bar{y}_{k-1}\|^2} \leq \frac{1}{(s_{k-1}^T \bar{y}_{k-1})^2}. \tag{4.17}$$

From (3.18) and (4.17), we have

$$|\theta_k| = \left| \frac{2(s_{k-1}^T \bar{y}_{k-1})^2}{(s_{k-1}^T \bar{y}_{k-1})^2 + \gamma \|s_{k-1}\|^2 \|\bar{y}_{k-1}\|^2} \right| \leq \left| \frac{2(s_{k-1}^T \bar{y}_{k-1})^2}{(s_{k-1}^T \bar{y}_{k-1})^2 (1+\gamma)} \right| = \frac{2}{1+\gamma}.$$

Setting $\frac{2}{1+\gamma} = v_2$, we get

$$|\theta_k| \leq v_2. \tag{4.18}$$

From (3.5) and (4.1), we obtain

$$\|\bar{y}_{k-1}\| \leq \|y_{k-1}\| + \varsigma \|s_{k-1}\| \leq L\|s_{k-1}\| + \varsigma \|s_{k-1}\| = (L + \varsigma)\|s_{k-1}\|. \tag{4.19}$$

Hence, using (3.4), (3.6), (4.18), (4.19), and the Cauchy Schwarz inequality, we have

$$\begin{aligned}\|d_k\| &\leq |\theta_k|\|F_k\| + |\theta_k|\frac{\|F_k\|\|\bar{y}_{k-1}\|\|s_{k-1}\|}{s_{k-1}^T\bar{y}_{k-1}} + |\theta_k|\frac{|\gamma|\|\bar{y}_{k-1}\|^2\|F_k\|\|s_{k-1}\|^2}{(s_{k-1}^T\bar{y}_{k-1})^2}\\ &\leq v_2\|F_k\| + v_2\frac{(L+\varsigma)\|F_k\|\|s_{k-1}\|^2}{\varsigma\|s_{k-1}\|^2} + v_2\frac{\gamma(L+\varsigma)^2\|F_k\|\|s_{k-1}\|^4}{\varsigma^2\|s_{k-1}\|^4}\\ &= v_2\|F_k\| + v_2\frac{(L+\varsigma)\|F_k\|}{\varsigma} + v_2\frac{\gamma(L+\varsigma)^2\|F_k\|}{\varsigma^2}\\ &\leq v_2\overline{u} + v_2\frac{(L+\varsigma)\overline{u}}{\varsigma} + v_2\frac{\gamma(L+\varsigma)^2\overline{u}}{\varsigma^2}\end{aligned}.$$

Setting $\Pi = v_2\overline{u} + v_2\frac{(L+\varsigma)\overline{u}}{\varsigma} + v_2\frac{\gamma(L+\varsigma)^2\overline{u}}{\varsigma^2}$, we have that

$$\|d_k\| \leq \Pi, \quad \forall k \geq 0. \tag{4.20}$$

Assuming that $\sigma_k \neq \beta$, from the definition of the step-size σ_k, $\frac{\sigma_k}{\rho}$ will not satisfy (3.20), i.e.,

$$-F(a_k + \frac{\sigma_k}{\rho}d_k)^T d_k < \mu\frac{\sigma_k}{\rho}\|d_k\|^2.$$

So, applying the inequality (3.17), Cauchy Schwarz inequality, and (4.1), we have

$$\begin{aligned}\psi\|F_k\|^2 \leq F_k^T d_k &= \left(F(a_k + \frac{\sigma_k}{\rho}d_k) - F_k\right)^T d_k - F\left(a_k + \frac{\sigma_k}{\rho}d_k\right)^T d_k\\ &\leq L\frac{\sigma_k}{\rho}\|d_k\|^2 + \mu\frac{\sigma_k}{\rho}\|d_k\|^2.\end{aligned}$$

Consequently, the second inequality implies that

$$\sigma_k \geq \frac{\psi\rho}{(L+\mu)}\frac{\|F_k\|^2}{\|d_k\|^2}.$$

Therefore, using (4.16) and (4.20), we get

$$\sigma_k\|d_k\| \geq \frac{\psi\rho}{(L+\mu)}\frac{\|F_k\|^2}{\|d_k\|} \geq \frac{\psi\rho}{(L+\mu)}\frac{v_1^2}{\Pi} > 0. \tag{4.21}$$

Clearly, (4.21) contradicts (4.14). □

5. Computational experiments and results discussions

This section examines the efficacy of Algorithm 1 labeled NHZIS for convenience by contrasting its performance with that of four iterative methods in the literature. For simplicity, we label these methods as SRCME [42], MHZM2 [25], CGD [4], and T2DFP [43], respectively. The same parameter selections made by the authors were also used in our experiments to implement the four schemes. The line search parameters for the NHZIS scheme are $\rho = 0.6$, $\beta = 1$, $\overline{\phi} = 1.7$, and $\mu = 10^{-4}$,

$\varsigma = 1.1$, $\gamma = 1.001$. MATLAB R2014a was used to generate the implementation codes on a Windows-based PC with the following specs: $(2.30GHzCPU, 4GBRAM)$. If the inequality $\|F(a_k)\| \leq 10^{-8}$ or $\|F(\vartheta_k)\| \leq 10^{-8}$ is reached or the iterations surpass 1000, the iterations for all five algorithms are set to end.

Additionally, the results of the experiments were displayed in Tables 1–3, where the labels Pnum, Nvars, Iguess, NIT, Fvalue, and Ptime denote test example number, dimension, initial guess, number of iterations, function evaluations, and CPU time, respectively. In addition, $\|F(a_k)\|$ indicates the norm value of the operator F at which a solution is attained while $***$ indicates failure of a scheme to find solution of any of the test examples.

The following test examples were employed for the experiments, where $F(a) = (f_1(a), f_2(a), ..., f_n(a))^T$.

Example 1. [44] with $\mathcal{B} = \mathbb{R}^n_+$
$f_i(a) = 2a_i - \sin|a_i|, \quad i = 1, 2, \ldots, n.$

Example 2. [3].
$f_1(a) = a_1 - e^{\left(\cos\left(\frac{a_1+a_2}{n+1}\right)\right)},$
$f_i(a) = a_i - e^{\left(\cos\left(\frac{a_{i-1}+a_i+a_{i+1}}{n+1}\right)\right)}, \quad i = 2, 3, \ldots, n-1,$
$f_n(a) = a_n - e^{\left(\cos\left(\frac{a_{n-1}+a_n}{n+1}\right)\right)},$
with $\mathcal{B} = \mathbb{R}^n_+$.

Example 3. Non-smooth Function [4].
$f_i(a) = a_i - \sin|a_i - 1|, \quad i = 1, 2, \ldots, n,$
where $\mathcal{B} = \left\{a \in \mathbb{R}^n : \sum_{i=1}^{n} a_i \leq n, \quad a_i \geq -1, \quad i = 1, 2, \ldots, n\right\}.$

Example 4. A modification of test example A1 in [27] with $\mathcal{B} = \mathbb{R}^n_+$ added to yield
$f_1(a) = e^{(\sin(a_1))} - 1,$
$f_i(a) = e^{(\sin(a_i))} + a_i - 1, \quad i = 2, \ldots, n.$

Example 5. A modification of the test example 4 with $\mathcal{B} = \mathbb{R}^n_+$ added to yield
$f_1(a) = \sin(a_1) + e^{(\sin(a_1))} - 1,$
$f_i(a) = \sin(a_i) + e^{(\sin(a_i))} + a_i - 1, \quad i = 2, \ldots, n.$

Example 6. [44] with $\mathcal{B} = \mathbb{R}^n_+$ added to yield
$f_i(x) = 2a_i - \sin(a_i), \quad i = 1, 2, \ldots, n.$

Example 7. Non-smooth function [44].
$f_i(a) = a_i - 2\sin|a_i - 1|, \quad i = 1, 2, \ldots, n,$
where $\mathcal{B} = \left\{a \in \mathbb{R}^n : \sum_{i=1}^{n} a_i \leq n, \quad a_i \geq -1, \quad i = 1, 2, \ldots, n\right\}.$

Example 8. A modification of the test example 5 with $\mathcal{B} = \mathbb{R}^n_+$ added to yield
$f_1(a) = 3a_1 + e^{(\sin(a_1))} - 1,$
$f_i(a) = 3a_i + e^{(\sin(a_i))} - 1, \quad i = 2, \ldots, n.$

Table 1. Numerical experiments for test examples 1–3.

Pnum	Nvars	NHZIS					SRCME				MHZM2				CGD				T2DFP			
		Iguess	NIT	Fvalue	Ptime	$\|F(a_k)$	NIT	Fvalue	Ptime	$\|F(a_k)$	NIT	Fvalue	Ptime	$\|F(a_k)$	NIT	Fvalue	Ptime	$\|F(a_k)$	NIT	Fvalue	Ptime	$\|F(a_k)$
1	5000	a_1	1	3	0.1141	0	27	30	0.1909	6.52E-09	67	69	0.2585	9.71E-09	84	169	0.1857	9.75E-09	1	2	0.1966	0
	5000	a_2	1	3	0.0165	0	32	35	1.0789	5.87E-09	79	81	0.0792	8.59E-09	99	199	0.7343	8.41E-09	1	2	0.0255	0
	5000	a_3	5	12	0.0145	5.12E-09	35	38	0.0199	6.17E-09	80	82	0.0849	9.28E-09	100	201	0.0763	9.87E-09	21	72	0.0217	0
	5000	a_4	4	9	0.0187	3.87E-09	31	34	0.0267	5.46E-09	77	79	0.0706	8.81E-09	96	193	0.0878	9.59E-09	1	2	0.0034	0
	5000	a_5	1	3	0.0067	0	31	34	0.0226	5.10E-09	77	79	0.0734	8.63E-09	96	193	0.0753	9.37E-09	1	2	0.0118	0
	5000	a_6	4	9	0.0068	4.29E-09	31	34	0.0195	5.47E-09	77	79	0.1158	8.82E-09	96	193	0.0726	9.60E-09	1	2	0.0049	0
	10000	a_1	1	3	0.0178	0	27	30	0.1010	6.53E-09	67	69	0.4253	9.71E-09	84	169	0.5769	9.75E-09	1	2	0.0070	0
	10000	a_2	1	3	0.0136	0	33	36	0.0955	9.31E-09	83	85	0.5273	8.99E-09	104	209	0.5164	8.71E-09	1	2	0.0098	0
	10000	a_3	5	14	0.0405	6.55E-09	36	39	0.1242	9.82E-09	84	86	0.4801	9.72E-09	106	213	0.5698	8.18E-09	19	81	0.1549	0
	10000	a_4	4	11	0.0403	5.15E-09	32	35	0.0984	8.66E-09	81	83	0.5390	9.23E-09	101	203	0.6091	9.94E-09	1	2	0.0096	0
	10000	a_5	1	3	0.0144	0	32	35	0.1072	8.07E-09	81	83	0.4903	9.04E-09	101	203	0.5781	9.71E-09	1	2	0.0098	0
	10000	a_6	4	11	0.0404	5.21E-09	32	35	0.1049	8.66E-09	81	83	0.5233	9.23E-09	101	203	0.5604	9.94E-09	1	2	0.0102	0
	50000	a_1	1	3	0.0335	0	27	30	0.3972	6.53E-09	67	69	1.6507	9.71E-09	84	169	1.7345	9.75E-09	1	2	0.0275	0
	50000	a_2	1	3	0.0485	0	35	38	0.5070	5.25E-09	86	88	2.1823	8.78E-09	107	215	2.2048	9.97E-09	1	2	0.0289	0
	50000	a_3	6	14	0.1598	5.38E-09	38	41	0.5177	5.57E-09	87	89	2.2326	9.48E-09	109	219	2.4064	9.37E-09	15	61	0.5333	0
	50000	a_4	5	11	0.1238	2.33E-09	33	36	0.5006	9.69E-09	84	86	2.0728	9.01E-09	105	211	2.3899	9.11E-09	1	2	0.0259	0
	50000	a_5	1	3	0.0380	0	33	36	0.5106	9.03E-09	84	86	2.1310	8.82E-09	105	211	2.2964	8.89E-09	1	2	0.0256	0
	50000	a_6	5	11	0.1733	2.34E-09	33	36	0.5340	9.69E-09	84	86	2.0521	9.01E-09	105	211	2.2028	9.11E-09	1	2	0.0266	0
2	5000	a_1	6	13	0.0168	6.34E-09	33	36	0.0271	5.98E-09	83	85	0.1059	8.45E-09	104	209	0.1409	8.03E-09	21	118	0.0572	5.75E-09
	5000	a_2	6	13	0.0134	4.18E-09	32	35	0.0358	7.90E-09	81	83	0.1133	9.69E-09	102	205	0.1064	8.29E-09	9	41	0.0233	3.45E-09
	5000	a_3	6	13	0.0192	2.83E-09	32	35	0.0386	5.44E-09	80	82	0.1083	8.80E-09	100	201	0.1208	8.92E-09	9	41	0.0201	2.94E-09
	5000	a_4	6	13	0.0223	5.23E-09	32	35	0.0269	9.87E-09	82	84	0.1316	9.19E-09	103	207	0.1508	8.29E-09	24	143	0.0608	4.43E-09
	5000	a_5	6	13	0.0177	5.22E-09	32	35	0.0271	9.85E-09	82	84	0.1167	9.17E-09	103	207	0.1976	8.27E-09	21	121	0.0449	2.57E-09
	5000	a_6	6	13	0.0155	5.23E-09	32	35	0.0267	9.87E-09	82	84	0.1470	9.19E-09	103	207	0.1139	8.28E-09	24	139	0.0476	8.90E-09
	10000	a_1	6	15	0.0630	7.88E-09	34	37	0.2376	9.49E-09	87	89	0.8050	8.88E-09	109	219	1.0510	8.36E-09	10	51	0.1425	7.06E-10
	10000	a_2	6	15	0.0664	5.19E-09	34	37	0.1813	6.25E-09	86	88	0.8006	7.71E-09	107	215	0.8719	8.60E-09	11	63	0.1724	2.77E-09
	10000	a_3	6	13	0.0683	8.94E-09	33	36	0.1768	8.60E-09	84	86	0.7515	9.22E-09	105	211	0.8292	9.25E-09	12	63	0.2541	8.72E-09
	10000	a_4	6	15	0.0746	6.49E-09	34	37	0.1797	7.81E-09	86	88	0.7843	9.64E-09	108	217	0.8845	8.60E-09	10	51	0.1675	4.58E-09
	10000	a_5	6	15	0.0875	6.48E-09	34	37	0.1694	7.80E-09	86	88	0.8173	9.62E-09	108	217	0.8947	8.58E-09	10	51	0.1390	4.81E-09
	10000	a_6	6	15	0.0653	6.49E-09	34	37	0.1905	7.81E-09	86	88	0.8667	9.64E-09	108	217	0.9368	8.60E-09	10	51	0.1493	4.58E-09
	50000	a_1	7	15	0.2856	9.05E-10	36	39	0.8040	5.31E-09	90	92	3.6657	8.67E-09	112	225	4.0940	9.57E-09	13	64	0.9151	7.62E-10
	50000	a_2	7	15	0.3411	5.96E-10	35	38	0.7907	6.99E-09	88	90	3.6350	9.92E-09	110	221	4.0128	9.85E-09	8	41	0.5441	3.02E-09
	50000	a_3	6	15	0.3035	7.99E-09	34	37	0.7598	9.62E-09	87	89	3.6139	9.00E-09	109	219	3.9202	8.47E-09	10	51	0.6808	6.01E-10
	50000	a_4	7	15	0.3295	7.45E-10	35	38	0.7767	8.73E-09	89	91	3.5874	9.41E-09	111	223	3.9880	9.85E-09	12	53	0.7243	7.79E-09
	50000	a_5	7	15	0.3059	7.43E-10	35	38	0.7797	8.72E-09	89	91	3.6261	9.39E-09	111	223	4.0881	9.83E-09	12	53	0.7465	7.67E-09
	50000	a_6	7	15	0.3015	7.45E-10	35	38	0.7930	8.73E-09	89	91	3.6679	9.41E-09	111	223	4.1094	9.85E-09	12	53	0.7692	7.79E-09
3	5000	a_1	11	34	0.0199	7.20E-09	35	38	0.0230	6.30E-09	37	39	0.0491	5.72E-09	48	97	0.0606	6.93E-09	19	113	0.0356	4.04E-09
	5000	a_2	11	33	0.0180	5.82E-09	36	40	0.0256	6.69E-09	37	39	0.0566	9.42E-09	49	99	0.0584	8.28E-09	42	253	0.0662	8.83E-09
	5000	a_3	17	50	0.0346	7.14E-09	38	41	0.0236	6.98E-09	49	77	0.0815	6.36E-09	50	100	0.0582	6.74E-09	15	87	0.0330	6.99E-10
	5000	a_4	11	34	0.0255	8.38E-09	36	39	0.0245	6.94E-09	35	37	0.0601	9.99E-09	46	93	0.0806	9.49E-09	48	277	0.0683	6.27E-09
	5000	a_5	11	34	0.0130	9.06E-09	35	38	0.0237	8.35E-09	35	37	0.0433	8.62E-09	46	93	0.0474	8.16E-09	20	120	0.0329	4.39E-09
	5000	a_6	11	34	0.0152	8.42E-09	36	39	0.0253	6.94E-09	35	37	0.0471	9.99E-09	46	93	0.1221	9.48E-09	37	211	0.0496	8.87E-09
	10000	a_1	11	37	0.0893	7.33E-09	36	39	0.1701	6.50E-09	39	41	0.4014	5.50E-09	50	101	0.3437	8.68E-09	35	163	0.3919	9.57E-09
	10000	a_2	11	36	0.0899	5.99E-09	38	42	0.1809	6.90E-09	39	41	0.3553	8.95E-09	52	105	0.3592	6.41E-09	24	147	0.3199	5.55E-09
	10000	a_3	17	53	0.1430	7.35E-09	40	43	0.1982	7.19E-09	51	79	0.5261	6.04E-09	52	104	0.3257	8.34E-09	29	157	0.3160	6.67E-09
	10000	a_4	11	37	0.0855	8.65E-09	38	41	0.1744	7.15E-09	37	39	0.3137	9.49E-09	49	99	0.3851	7.34E-09	37	197	0.4278	9.16E-09
	10000	a_5	11	37	0.1310	9.33E-09	37	40	0.1591	8.60E-09	37	39	0.3093	8.19E-09	49	99	0.3177	6.32E-09	30	157	0.3185	1.09E-09
	10000	a_6	11	37	0.0970	8.65E-09	38	41	0.1797	7.15E-09	37	39	0.3214	9.49E-09	49	99	0.4046	7.34E-09	31	144	0.3171	6.39E-09
	50000	a_1	12	37	0.3849	7.36E-09	36	39	0.7054	9.76E-09	40	42	1.3888	6.75E-09	52	105	1.3225	7.61E-09	48	257	2.1627	5.88E-09
	50000	a_2	12	36	0.4197	6.02E-09	39	43	0.7408	8.81E-09	41	43	1.4065	6.01E-09	53	107	1.3128	8.97E-09	29	157	1.2995	7.35E-09
	50000	a_3	18	53	0.5459	7.39E-09	41	44	0.7583	9.18E-09	52	80	2.0336	7.41E-09	54	108	1.3401	7.29E-09	18	87	0.7757	7.94E-09
	50000	a_4	12	37	0.3519	8.69E-09	39	42	0.6916	9.13E-09	39	41	1.3129	6.37E-09	51	103	1.2792	6.43E-09	33	164	1.4487	3.77E-09
	50000	a_5	12	37	0.3730	9.38E-09	39	42	0.7428	6.27E-09	39	41	1.2954	5.50E-09	50	101	1.2506	8.84E-09	24	121	1.0410	5.30E-09
	50000	a_6	12	37	0.3566	8.69E-09	39	42	0.7366	9.13E-09	39	41	1.2801	6.37E-09	51	103	1.2985	6.43E-09	31	160	1.3997	4.34E-09

Table 2. Numerical experiments for test examples 1–3.

Pnum	Nvars	NHZIS					SRCME				MHZM2				CGD				T2DFP			
		Iguess	NIT	Fvalue	Ptime	$\|F(a_k)$	NIT	Fvalue	Ptime	$\|F(a_k)$	NIT	Fvalue	Ptime	$\|F(a_k)$	NIT	Fvalue	Ptime	$\|F(a_k)$	NIT	Fvalue	Ptime	$\|F(a_k)$
4	5000	a_1	11	31	0.0157	1.22E-09	31	33	0.0284	5.49E-09	62	64	0.0931	8.22E-09	80	161	0.0709	9.33E-09	22	115	0.0304	0
	5000	a_2	1	4	0.0153	0	40	42	0.0228	5.71E-09	48	50	0.0524	9.81E-09	73	147	0.0748	9.15E-09	11	48	0.0190	0
	5000	a_3	18	59	0.0347	0	43	46	0.0322	8.04E-09	77	90	0.0758	9.97E-09	86	173	0.1040	9.98E-09	22	107	0.0392	0
	5000	a_4	1	4	0.0094	0	38	41	0.0303	6.66E-09	49	51	0.0519	8.70E-09	73	147	0.0724	8.25E-09	3	7	0.0051	0
	5000	a_5	1	4	0.0060	0	38	40	0.0227	8.88E-09	47	49	0.0637	9.90E-09	71	143	0.0576	9.23E-09	3	7	0.0062	0
	5000	a_6	1	4	0.0061	0	38	41	0.0224	5.14E-09	33	35	0.0454	7.79E-09	44	89	0.0455	6.68E-09	3	7	0.0054	0
	10000	a_1	11	31	0.1031	1.72E-09	31	33	0.1030	5.50E-09	62	64	0.4493	8.21E-09	80	161	0.4478	9.33E-09	13	57	0.1143	0
	10000	a_2	1	4	0.0152	0	41	44	0.1406	6.17E-09	45	47	0.3385	7.66E-09	70	141	0.4123	9.63E-09	16	70	0.1508	0
	10000	a_3	9	27	0.0735	0	46	49	0.1598	6.95E-09	77	90	0.5178	9.93E-09	84	169	0.5297	8.02E-09	20	104	0.2061	0
	10000	a_4	1	4	0.0174	0	40	43	0.1649	6.67E-09	45	47	0.3022	8.75E-09	70	141	0.4298	8.68E-09	4	9	0.0394	0
	10000	a_5	1	4	0.0222	0	40	43	0.1490	5.67E-09	44	46	0.3386	7.76E-09	68	137	0.4379	9.72E-09	4	9	0.0338	0
	10000	a_6	1	4	0.0192	0	40	43	0.1417	5.42E-09	35	37	0.2585	6.58E-09	46	93	0.2944	7.48E-09	4	9	0.0314	0
	50000	a_1	11	31	0.3369	1.74E-09	31	33	0.4380	5.50E-09	62	64	1.7456	8.21E-09	80	161	1.7547	9.33E-09	11	43	0.4384	0
	50000	a_2	1	4	0.0477	0	42	45	0.6627	7.30E-09	42	44	1.2216	9.99E-09	68	137	1.7262	9.78E-09	5	11	0.1726	0
	50000	a_3	9	27	0.3233	0	48	51	0.7167	6.48E-09	77	90	2.1024	9.93E-09	82	165	1.9185	8.06E-09	20	101	0.8991	0
	50000	a_4	1	4	0.0560	0	42	44	0.6163	8.94E-09	43	45	1.1998	7.83E-09	68	137	1.5715	8.82E-09	8	29	0.3164	0
	50000	a_5	1	4	0.0465	0	42	44	0.6047	7.76E-09	42	44	1.1984	7.31E-09	66	133	1.5335	9.88E-09	23	123	1.0439	8.87E-09
	50000	a_6	1	4	0.0431	0	42	44	0.6128	8.57E-09	36	38	1.0654	7.61E-09	48	97	1.1497	6.02E-09	8	34	0.3233	4.47E-09
5	5000	a_1	2	8	0.0126	0	31	35	0.0314	6.22E-09	7	19	0.0231	0	31	63	0.0393	6.94E-09	5	18	0.0085	0
	5000	a_2	6	25	0.0146	0	47	50	0.0386	7.60E-09	5	17	0.0229	0	26	53	0.0327	7.29E-09	5	16	0.0092	0
	5000	a_3	6	23	0.0226	0	46	53	0.0298	6.91E-09	32	45	0.0485	5.66E-09	28	57	0.0345	8.83E-09	31	179	0.0509	9.82E-09
	5000	a_4	1	5	0.0088	0	42	45	0.0373	9.88E-09	6	19	0.0184	0	25	51	0.0428	9.15E-09	1	3	0.0041	0
	5000	a_5	1	5	0.0051	0	38	42	0.0292	4.81E-09	6	21	0.0183	0	25	51	0.0430	8.81E-09	1	3	0.0038	0
	5000	a_6	1	5	0.0099	0	42	46	0.0270	6.03E-09	6	19	0.0246	0	25	51	0.0279	8.87E-09	1	3	0.0039	0
	10000	a_1	2	8	0.0290	0	31	35	0.1424	6.23E-09	7	19	0.1152	0	31	63	0.2376	6.92E-09	5	18	0.0531	0
	10000	a_2	6	25	0.0725	0	49	53	0.2502	4.99E-09	5	17	0.1016	0	27	55	0.2217	9.10E-09	5	16	0.0501	0
	10000	a_3	6	23	0.0852	0	48	55	0.2286	7.18E-09	36	49	0.4141	7.53E-09	29	59	0.2627	9.42E-09	6	17	0.0620	0
	10000	a_4	1	5	0.0192	0	44	48	0.2255	6.90E-09	6	19	0.0841	0	27	55	0.2215	4.50E-09	1	3	0.0135	0
	10000	a_5	1	5	0.0233	0	40	44	0.2093	6.23E-09	6	21	0.1260	0	27	55	0.2397	4.38E-09	1	3	0.0136	0
	10000	a_6	1	5	0.0265	0	44	48	0.2191	7.13E-09	6	19	0.0939	0	27	55	0.2074	4.49E-09	1	3	0.0150	0
	50000	a_1	2	8	0.1060	0	31	35	0.6039	6.23E-09	7	19	0.4280	0	31	63	0.9298	6.92E-09	5	18	0.2577	0
	50000	a_2	6	25	0.3382	0	51	54	0.9556	9.29E-09	5	17	0.4317	0	28	57	0.9475	8.13E-09	5	16	0.2211	0
	50000	a_3	6	23	0.3197	0	50	57	0.9686	5.92E-09	38	51	1.4234	5.57E-09	30	61	1.0497	8.31E-09	6	17	0.2754	0
	50000	a_4	1	5	0.0555	0	46	50	0.8185	5.93E-09	6	19	0.4192	0	28	57	0.9010	4.02E-09	1	3	0.0442	0
	50000	a_5	1	5	0.0627	0	42	46	0.7226	5.28E-09	6	21	0.3990	0	27	55	0.8342	9.77E-09	1	3	0.0473	0
	50000	a_6	1	5	0.0768	0	46	50	0.8191	5.98E-09	6	19	0.3880	0	28	57	0.8708	4.01E-09	1	3	0.0476	0
6	5000	a_1	1	4	0.0086	0	34	36	0.0200	7.95E-09	29	31	0.0400	9.59E-09	39	79	0.0438	7.26E-09	2	5	0.0064	0
	5000	a_2	1	4	0.0074	0	40	43	0.0219	5.17E-09	34	36	0.0719	8.82E-09	45	91	0.0427	8.56E-09	3	7	0.0048	0
	5000	a_3	4	14	0.0122	9.66E-09	40	44	0.0256	6.87E-09	35	37	0.0344	6.76E-09	46	93	0.0468	7.94E-09	1	3	0.0052	0
	5000	a_4	1	4	0.0052	0	38	41	0.0197	4.79E-09	33	35	0.0484	9.82E-09	44	89	0.0436	8.07E-09	3	7	0.0048	0
	5000	a_5	1	4	0.0068	0	38	40	0.0225	7.55E-09	33	35	0.0329	9.59E-09	44	89	0.0353	7.86E-09	3	7	0.0051	0
	5000	a_6	1	4	0.0071	0	38	41	0.0279	4.80E-09	33	35	0.0401	9.84E-09	44	89	0.0466	8.08E-09	3	7	0.0060	0
	10000	a_1	1	4	0.0175	0	34	36	0.0968	7.95E-09	29	31	0.1994	9.59E-09	39	79	0.2255	7.27E-09	2	5	0.0171	0
	10000	a_2	1	4	0.0158	0	42	45	0.1317	5.45E-09	36	38	0.2357	7.46E-09	47	95	0.2385	9.74E-09	4	9	0.0333	0
	10000	a_3	4	17	0.0483	8.56E-09	42	46	0.1329	7.24E-09	37	39	0.2450	5.72E-09	48	97	0.2601	9.04E-09	1	3	0.0125	0
	10000	a_4	1	4	0.0179	0	40	43	0.1114	5.05E-09	35	37	0.2342	8.31E-09	46	93	0.2262	9.19E-09	4	9	0.0417	0
	10000	a_5	1	4	0.0187	0	40	42	0.1298	7.96E-09	35	37	0.2215	8.11E-09	46	93	0.2555	8.95E-09	4	9	0.0283	0
	10000	a_6	1	4	0.0143	0	40	43	0.1427	5.05E-09	35	37	0.2339	8.31E-09	46	93	0.2730	9.19E-09	4	9	0.0271	0
	50000	a_1	1	4	0.0356	0	34	36	0.4638	7.95E-09	29	31	0.7782	9.59E-09	39	79	0.8428	7.27E-09	2	5	0.0521	0
	50000	a_2	1	4	0.0417	0	44	46	0.5988	8.62E-09	37	39	0.9582	8.63E-09	49	99	1.0720	7.84E-09	5	11	0.1416	0
	50000	a_3	5	17	0.1858	1.48E-09	44	48	0.5718	5.40E-09	38	40	1.0079	6.61E-09	50	101	1.1253	7.27E-09	1	3	0.0418	0
	50000	a_4	1	4	0.0431	0	42	44	0.5562	7.99E-09	36	38	0.9295	9.61E-09	48	97	1.1012	7.40E-09	5	11	0.1093	0
	50000	a_5	1	4	0.0512	0	40	43	0.5921	8.39E-09	36	38	0.8916	9.38E-09	48	97	1.0763	7.21E-09	5	11	0.1182	0
	50000	a_6	1	4	0.0374	0	42	44	0.5458	7.99E-09	36	38	0.9154	9.61E-09	48	97	1.0053	7.40E-09	5	11	0.1342	0

Table 3. Numerical experiments for test examples 7 and 8.

Pnum	Nvars		NHZIS				SRCME				MHZM2				CGD				T2DFP			
		Iguess	NIT	Fvalue	Ptime	$\|F(a_k)$	NIT	Fvalue	Ptime	$\|F(a_k)$	NIT	Fvalue	Ptime	$\|F(a_k)$	NIT	Fvalue	Ptime	$\|F(a_k)$	NIT	Fvalue	Ptime	$\|F(a_k)$
7	5000	a_1	9	36	0.0221	2.67E-09	40	44	0.0440	7.40E-09	57	178	0.0846	4.05E-09	28	57	0.0380	4.23E-09	37	213	0.0493	8.85E-09
	5000	a_2	21	82	0.0399	5.09E-09	41	44	0.0299	8.11E-09	* * * *	* * * *	* * * *	* * * *	30	60	0.0359	4.98E-09	58	265	0.0668	8.15E-09
	5000	a_3	21	79	0.0259	6.61E-09	47	57	0.0359	7.70E-09	54	223	0.0874	8.56E-09	34	69	0.0363	6.88E-09	46	206	0.0555	9.98E-09
	5000	a_4	17	66	0.0271	6.87E-09	41	45	0.0338	6.73E-09	* * * *	* * * *	* * * *	* * * *	27	55	0.0410	4.63E-09	44	209	0.0593	9.67E-09
	5000	a_5	10	40	0.0167	7.07E-09	39	43	0.0289	9.77E-09	71	241	0.1003	9.09E-09	26	53	0.0416	9.68E-09	26	127	0.0348	9.69E-09
	5000	a_6	19	78	0.0356	5.98E-09	41	45	0.0381	6.72E-09	38	124	0.0806	3.94E-09	27	55	0.0271	4.62E-09	33	173	0.0441	8.64E-09
	10000	a_1	9	40	0.1117	8.39E-09	41	45	0.1807	8.25E-09	51	156	0.6917	9.78E-09	29	59	0.2063	5.71E-09	31	169	0.3685	7.85E-09
	10000	a_2	22	82	0.1791	2.32E-09	43	46	0.2040	9.52E-09	* * * *	* * * *	* * * *	* * * *	31	62	0.2007	6.75E-09	30	168	0.3649	9.30E-09
	10000	a_3	21	83	0.1667	7.86E-09	49	59	0.2407	9.04E-09	* * * *	* * * *	* * * *	* * * *	35	71	0.2173	9.47E-09	56	276	0.5509	6.40E-09
	10000	a_4	18	71	0.1630	5.56E-09	43	47	0.2348	7.89E-09	* * * *	* * * *	* * * *	* * * *	28	57	0.2347	6.18E-09	29	147	0.3185	8.41E-09
	10000	a_5	10	44	0.0863	8.41E-09	42	46	0.1917	6.99E-09	73	207	0.7459	5.25E-09	28	57	0.1725	5.47E-09	26	152	0.3348	4.88E-09
	10000	a_6	18	71	0.1706	5.87E-09	43	47	0.2277	7.89E-09	68	238	0.8480	8.55E-09	28	57	0.2165	6.18E-09	32	161	0.3981	7.81E-09
	50000	a_1	10	40	0.3997	3.26E-09	42	46	0.8813	7.54E-09	51	174	2.6817	6.16E-09	30	61	0.7516	5.40E-09	26	150	1.2861	9.50E-09
	50000	a_2	22	82	0.7375	5.19E-09	45	48	0.8801	7.90E-09	* * * *	* * * *	* * * *	* * * *	32	64	0.8765	6.40E-09	46	205	1.8182	9.20E-09
	50000	a_3	22	83	0.7306	2.83E-09	51	61	0.9822	7.51E-09	111	504	6.8228	7.46E-09	36	73	0.9824	9.03E-09	39	184	1.5904	7.13E-09
	50000	a_4	18	75	0.6630	4.84E-09	45	49	0.8919	6.55E-09	* * * *	* * * *	* * * *	* * * *	29	59	0.7449	5.84E-09	43	212	2.0235	4.95E-09
	50000	a_5	11	44	0.3935	3.03E-09	43	47	0.8260	9.53E-09	87	286	4.2958	7.81E-09	29	59	0.7841	5.17E-09	39	183	1.6071	6.06E-09
	50000	a_6	18	75	0.6551	4.90E-09	45	49	0.9021	6.55E-09	68	258	3.8364	9.47E-09	29	59	0.7530	5.84E-09	26	126	1.1160	7.05E-09
8	5000	a_1	1	5	0.0097	0	39	43	0.0230	9.67E-09	4	17	0.0172	0	37	93	0.0370	8.61E-09	1	3	0.0039	0
	5000	a_2	1	5	0.0071	0	47	51	0.0461	5.76E-09	4	17	0.0124	0	52	131	0.0801	6.91E-09	1	3	0.0055	0
	5000	a_3	12	60	0.0284	0	50	55	0.0514	7.20E-09	4	25	0.0172	0	67	171	0.0625	4.83E-09	14	67	0.0302	0
	5000	a_4	1	5	0.0053	0	46	49	0.0241	9.01E-09	4	17	0.0182	0	65	160	0.0626	8.89E-09	1	3	0.0050	0
	5000	a_5	1	5	0.0049	0	46	49	0.0356	9.47E-09	4	17	0.0109	0	58	143	0.0614	9.46E-09	1	3	0.0051	0
	5000	a_6	1	5	0.0062	0	46	49	0.0287	9.01E-09	4	17	0.0120	0	65	160	0.0594	8.84E-09	1	3	0.0035	0
	10000	a_1	1	5	0.0179	0	39	43	0.1460	9.68E-09	4	17	0.0738	0	46	115	0.3429	7.82E-09	1	3	0.0121	0
	10000	a_2	1	5	0.0184	0	49	53	0.1955	7.29E-09	4	17	0.0764	0	53	137	0.3912	5.36E-09	1	3	0.0127	0
	10000	a_3	12	60	0.1411	0	52	57	0.1896	9.11E-09	4	25	0.0888	0	57	139	0.4555	5.82E-09	27	167	0.3610	6.06E-09
	10000	a_4	1	5	0.0203	0	48	52	0.1855	5.10E-09	4	17	0.0634	0	67	163	0.4874	9.79E-09	1	3	0.0120	0
	10000	a_5	1	5	0.0194	0	48	52	0.1716	5.36E-09	4	17	0.0788	0	59	145	0.4217	7.94E-09	1	3	0.0118	0
	10000	a_6	1	5	0.0172	0	48	52	0.1765	5.10E-09	4	17	0.0634	0	67	163	0.4472	9.79E-09	1	3	0.0137	0
	50000	a_1	1	5	0.0607	0	39	43	0.5958	9.69E-09	4	17	0.2391	0	48	120	1.1925	8.02E-09	1	3	0.0360	0
	50000	a_2	1	5	0.0551	0	51	55	0.7865	6.52E-09	4	17	0.2704	0	63	152	1.6430	9.30E-09	1	3	0.0403	0
	50000	a_3	12	60	0.5343	0	54	59	0.7998	8.15E-09	4	25	0.3823	0	60	147	1.6092	8.64E-09	11	52	0.5088	0
	50000	a_4	1	5	0.0686	0	50	54	0.7387	4.56E-09	4	17	0.2701	0	70	171	1.7722	8.85E-09	1	3	0.0362	0
	50000	a_5	1	5	0.0466	0	50	54	0.7292	4.79E-09	4	17	0.2689	0	54	133	1.4203	7.81E-09	1	3	0.0357	0
	50000	a_6	1	5	0.0554	0	50	54	0.7350	4.56E-09	4	17	0.2690	0	70	171	1.7888	8.85E-09	1	3	0.0972	0

The experiments were performed with variables 1000, 10000, and 50000, with the following six initial points:

$a_1 = \left(1, \frac{1}{2}, ..., \frac{1}{n}\right)^T$, $a_2 = \left(\frac{1}{2}, \frac{3}{2}, ..., -\frac{[(-1)^n-2]}{2}\right)^T$, $a_3 = \left(1, 3, ..., ..., -\frac{-2[(-1)^n-2]}{2}\right)^T$,
$a_4 = \left(\frac{n-1}{n}, \frac{n-2}{n}, ..., 0\right)^T$, $a_5 = \left(\frac{1}{4}, \frac{3}{4}, ..., \frac{-[(-1)^n-2]}{4}\right)^T$, $a_6 = \left(\frac{1}{n}, \frac{2}{n}, ..., 1\right)^T$.

To provide an insight into the numerical performance of all the methods used in the experiments, a summary of the results in Tables 1–3, which are based on number of iterations, function evaluations, and CPU time, are drawn in Table 4. The results indicate that the NHZIS scheme outperforms the SCRME, MHZM2, CGD, and T2DFP methods in all three metrics considered. It is observed from Table 4 that NHZIS solved 91 (63.19%) of the test examples with fewer iterations than the SRCME, MHZM2, CGD, and T2DFP solvers, which recorded 0 (0%), 3 (2.09%), 0 (0%), and 10 (6.95%), respectively. It's interesting to note that 40 (27.77%) of the test examples were solved by more than one of the five algorithms with least iterations, which are designated as "TIES" in the summary table.

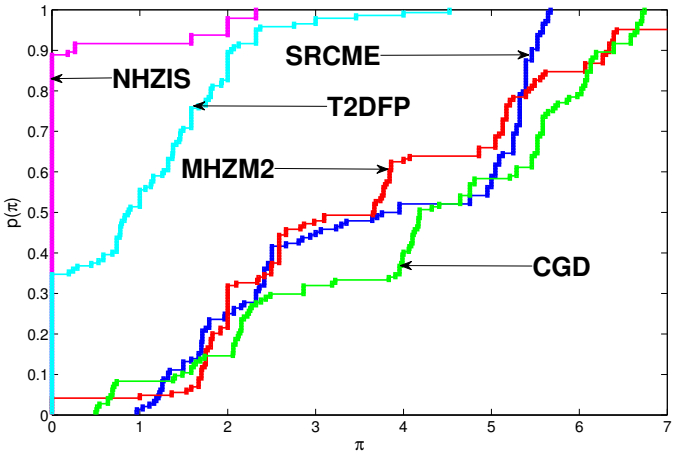

Figure 1. Dolan and Moré profile for iterations.

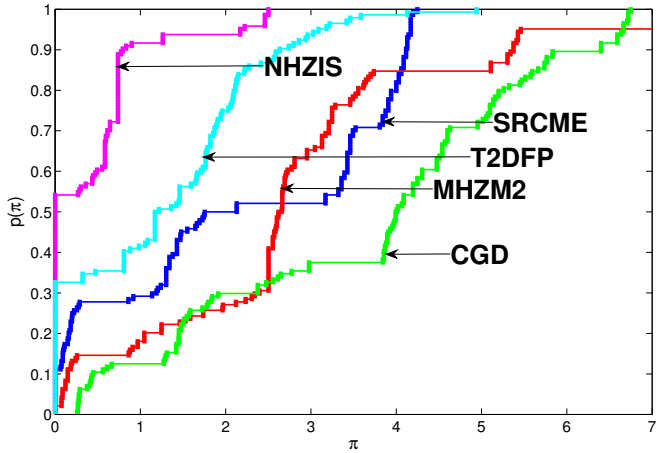

Figure 2. Dolan and Moré profile for function evaluations.

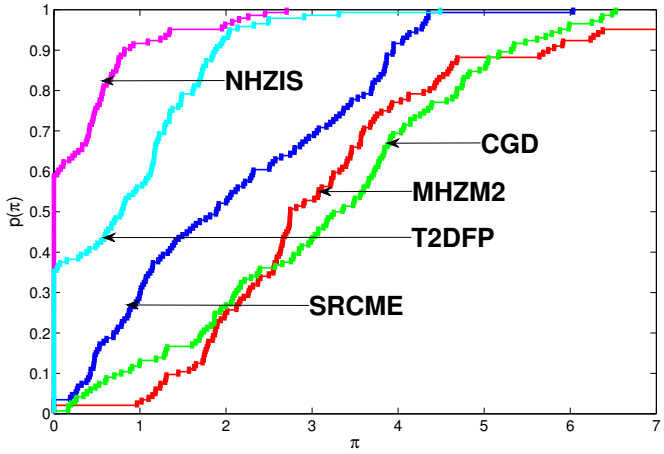

Figure 3. Dolan and Mor*é* profile for processing time.

Table 4. Summary of the results presented in Tables 1–3.

Method	NIT	Percentage	Fvalue	Percentage	Ptime	Percentage
NHZIS	91	63.19%	78	54.16%	84	58.33%
SRCME	0	0%	16	11.11%	5	3.47%
MHZM2	3	2.09%	3	2.09%	3	2.09%
CGD	0	0%	0	0%	1	0.69%
T2DFP	10	6.95%	47	32.64%	51	35.42%
TIES	40	27.77%	0	0%	0	0

Regarding least function evaluations, Table 4 shows that the NHZIS scheme solved 78 (54.16%) of the test examples, while SRCME, MHZM2, CGD, and T2DFP recorded 16 (11.11%), 3 (2.09%), 0 (0%), and 47 (33.64%), respectively. The summary table also indicates that NHZIS solved 84 (58.33%) of the test examples with the least amount of processing time compared to SRCME, MHZM2, CGD, and T2DFP that recorded 5 (3.47%), 3 (2.09%), 1 (0.69%), and 51 (35.42%) respectively.

Furthermore, the data presented in Tables 1–3 is plotted in Figures 1–3 for the three aforementioned performance metrics using the performance tool designed by Dolan and Moré [45]. It can be seen from each of the three figures that NHZIS solved more of the test examples with least values of each metric considered than SRCME, MHZM2, CGD, and T2DFP. Therefore, it can be inferred from the above discussion that the NHZIS scheme performs better than the other four methods in solving the constrained variant of (1.1).

6. Application of NHZIS in compressed sensing

6.1. A concept's insight

Over the years, the idea of digital image processing which aims to enhance the quality of the images being considered, has gained popularity in a variety of applications (see Ref. [46–48]). One common

example is in compressed sensing, where the goal is to minimize the following $\ell_1 - \ell_2$ *norm* problem in order to obtain sparse solutions to ill-conditioned linear systems of equations:

$$\min_a \frac{1}{2}||Na - q||_2^2 + \varpi||a||_1, \tag{6.1}$$

where $\varpi \geq 0$, $a \in \mathbb{R}^n$, and $q \in \mathbb{R}^k$ represents an observed value. The matrix $N \in \mathbb{R}^{n\times k}$ (with $k \ll n$) denotes a linear mapping. The terms $||a||_1$ and $||a||_2$ refer to the ℓ_1 and ℓ_2 norms, respectively. It is evident that (6.1) represents the unconstrained optimization problem commonly known as the ℓ_1-regularized least squares problem. There are numerous methods for solving (6.1) (see [49–51]), with gradient-based methods being among the most popular. In [52], Figueiredo et al. reformulated (6.1) as a convex quadratic problem, where the vector $a \in \mathbb{R}^n$ is divided into two parts as

$$a = u - w, \quad u \geq 0, \quad w \geq 0, \quad u, w \in \mathbb{R}^n. \tag{6.2}$$

Let $u_i = (a_i)_+, \quad w_i = (-a_i)_+ \quad \forall i = 1, 2, ..., n$, where $(.)_+$ denotes a positive operator defined as $(.)_+ = \max\{0, a\}$. Applying the definition of the $\ell_1 - norm$, we have $||a||_1 = A_n^T u + A_n^T w$. Here, $A_n = (1, 1, ..., 1)^T \in \mathbb{R}^n$. This representation reformulates (6.1) as

$$\min_{u,w} \frac{1}{2}||N(u - w) - q||_2^2 + \varpi A_n u + \varpi A_n w, \ \ u, w \geq 0. \tag{6.3}$$

Using the concept in [52], (6.3) becomes

$$\min_\lambda \frac{1}{2}\lambda^T W\lambda + D^T W\lambda, \quad \lambda \geq 0, \tag{6.4}$$

which represents a quadratic program problem where

$$\lambda = \begin{pmatrix} u \\ w \end{pmatrix}, \quad D = \varpi A_{2n} + \begin{pmatrix} -h \\ h \end{pmatrix}, \quad h = N^T q, \quad W = \begin{pmatrix} N^T N & -N^T N \\ -N^T N & N^T N \end{pmatrix}, \tag{6.5}$$

where the matrix W is positive semi-definite. Therefore, (6.4) is a convex quadratic programming problem, which is equivalent to

$$F(\lambda) = \min\{\lambda, W\lambda + D\} = 0, \tag{6.6}$$

where the function F is vector-valued, monotone, and Lipschitz continuous. Hence, by ([50, 53]), the NHZIS scheme can be used to solve it.

6.2. Numerical experiments

Here, we further illustrate the efficacy of the NHZIS scheme by running two compressed sensing tests. In both tests, we compare performance of NHZIS with that of CGD [4], PCG [3], SRCME [42], and T2DFP [43], where parameters of each scheme remain as used in the respective papers, with $\phi = 1.6$ for NHZIS. We begin by applying the five algorithms to recover a sparse signal with n lengths from k observed values. The mean of square error (MSE) to the original signal $\tilde{a}$, namely,

$$MSE = \frac{1}{n}||\tilde{a} - \bar{a}||^2, \tag{6.7}$$

is used to calculate restoration quality. Furthermore, the signal size is selected as $n = 2^{12}$ and $k = 2^{10}$, whereas the original signal includes 2^5 randomly nonzero components. In addition, Matlab's command randn(k,n) creates the Gaussian matrix N. The measurement k is disturbed by noise, i.e.,

$$k = N\bar{a} + \omega, \tag{6.8}$$

where ω represents the Gaussian noise, which is distributed as $\bar{N}(0, 10^{-4})$. Moreover, we use $f(a) = \frac{1}{2}\|Na - q\|_2^2 + \varpi\|a\|_1$ for the merit function.

Also, the measurement signal namely, $a_0 = N^T q$, is employed to start the experiment, which terminates when

$$\frac{\|f_k - f_{k-1}\|}{\|f_{k-1}\|} < 10^{-5}, \tag{6.9}$$

where f_k is the function value at a_k.

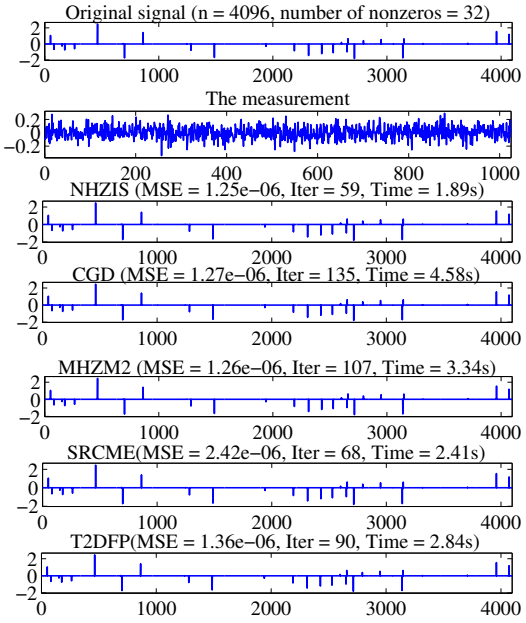

Figure 4. The Original, measured and recovered signals.

The sparse signal reconstruction test results are given in Figures 4 and 5, where the former shows that the disturbed signal was reconstructed almost exactly as the original one by NHZIS, CGD, PCG, SRCME, and T2DFP. Besides, it can be seen from Figures 4 and 5 that the quality of reconstruction as given by MSE is significantly better for NHZIS than CGD, PCG, SRCME, and T2DFP, where NHZIS recorded 1.25×10^{-6} and the latter recorded 1.27×10^{-6}, 1.26×10^{-6}, 2.42×10^{-6}, and 1.36×10^{-6}. Also, for the reconstruction process, Figures 4 and 5 shows that NHZIS yields the least number of iterations (59) and CPU time (1.89) compared to CGD, PCG, SRCME, and T2DFP. Furthermore, to obtain a statistically stronger result, we carry out more trials with fourteen different noise samples. Results of the experiments are given in Table 5, where v represents the number of nonzero elements with the bold and underlined values indicating the most efficient scheme. By these results, we conclude that NHZIS is efficient for reconstructing signals from disturbed ones.

Table 5. Sparse signal reconstruction results with different noise samples for NHZIS, CGD, PCG, SRCME, and T2DFP.

Size of each problem			NHZIS			CGD			PCG			SRCME			T2DFP		
n	k	v	MSE	**NIT**	Ptime	MSE	**NIT**	Ptime	MSE	**NIT**	Ptime	MSE	**NIT**	Ptime	MSE	**NIT**	Ptime
1024	256	32	**7.405e-06**	**101**	**0.27**	1.002e-03	102	0.19	1.816e-05	178	0.34	8.559e-06	128	0.28	1.405e-05	261	0.50
1536	384	48	**4.108e-06**	**84**	**0.44**	2.753e-04	93	0.41	8.281e-06	152	0.72	5.226e-06	106	0.52	9.146e-06	209	1.30
2048	512	64	**5.882e-06**	**71**	**0.66**	1.535e-04	142	1.31	6.369e-06	166	1.67	6.836e-06	106	0.94	5.920e-06	256	2.28
2560	640	80	7.241e-06	**68**	**0.88**	1.929e-04	117	1.59	1.339e-05	131	1.69	8.229e-06	112	1.70	**7.223e-06**	231	2.95
3072	768	96	**1.503e-05**	**89**	**1.95**	3.576e-04	123	2.70	3.677e-04	144	2.77	2.939e-05	104	2.34	1.649e-05	234	4.45
3584	896	112	**8.510e-06**	**76**	**1.78**	3.307e-04	133	3.38	1.758e-05	134	3.28	1.128e-05	110	2.67	8.595e-06	240	6.22
4096	1024	128	**1.012e-05**	**86**	**3.09**	5.027e-04	126	4.06	3.260e-05	99	3.42	1.186e-05	113	3.92	1.689e-05	219	7.25
4608	1152	144	6.862e-06	**82**	**3.39**	2.538e-04	124	4.89	1.150e-05	150	5.91	9.294e-06	107	4.03	**6.796e-06**	258	10.06
5120	1280	160	**1.136e-05**	**90**	**4.53**	9.363e-04	99	5.06	1.517e-05	147	7.16	1.223e-05	116	5.83	1.266e-05	262	13.55
5632	1408	176	9.691e-06	**87**	**5.06**	2.710e-04	169	9.44	1.790e-05	138	7.94	9.643e-06	128	7.19	**9.496e-06**	275	16.34
6144	1536	192	**8.600e-06**	**88**	**6.23**	6.795e-04	111	10.55	9.479e-06	190	17.33	1.079e-05	118	8.81	9.683e-06	266	21.52
6656	1664	208	**1.062e-05**	**85**	**6.75**	4.667e-04	134	11.33	1.633e-05	166	13.17	2.086e-05	110	8.75	1.204e-05	254	20.27
7168	1792	224	**1.023e-05**	**88**	**10.13**	8.041e-04	128	13.86	2.014e-05	164	16.98	2.103e-05	90	9.00	1.117e-05	250	25.38
7680	1920	240	1.133e-05	**85**	**9.16**	6.333e-04	125	13.94	7.339e-04	93	10.19	1.206e-05	112	12.27	**1.120e-05**	272	29.61

Table 6. Image recovery results for NHZIS, CGD, PCG, SRCME, and T2DFP.

Images with dimension	NHZIS				CGD				PCG				SRCME				T2DFP			
	MSE	SNR	PSNR	SSIM	MSE	SNR	PSNR	SSIM	MSE	SNR	PSNR	SSIM	MSE	SNR	PSNR	SSIM	MSE	SNR	PSNR	SSIM
Boat.png(512×512)	**6.6058e+01**	**24.59**	**29.93**	**0.84**	2.7435e+02	18.41	23.75	0.73	7.4679e+01	24.06	29.40	0.82	6.9766e+01	24.35	29.69	0.83	9.2687e+01	23.12	28.46	0.80
Girl.bmp(512×512)	**1.2856e+02**	**22.39**	**27.07**	**0.79**	2.5860e+02	19.36	23.86	0.71	1.4377e+02	21.91	26.55	0.77	1.3251e+02	22.26	26.92	**0.79**	1.6014e+02	21.44	26.09	0.76
Girlface.bmp(512×512)	**2.7776e+01**	**25.41**	**32.09**	**0.92**	1.0892e+03	9.48	15.95	0.77	3.1690e+01	24.84	31.54	0.90	3.0262e+01	25.04	31.80	**0.92**	3.5644e+01	24.33	30.96	0.90
Peppers.bmp(256×256)	9.5924e+01	22.59	27.27	0.85	1.2013e+02	21.61	26.27	0.83	8.4591e+01	23.14	27.81	0.86	**7.8079e+01**	**23.49**	**28.24**	**0.87**	1.1198e+02	21.92	26.65	0.83

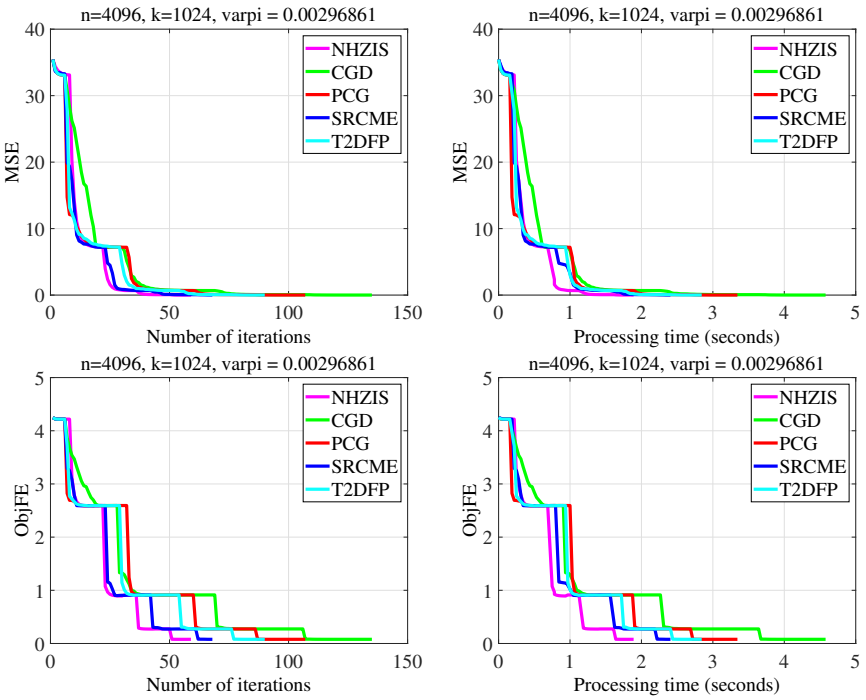

Figure 5. Test results of NHZIS, CGD, PCG, SRCME, and T2DFP.

The performance of the NHZIS scheme in image de-blurring challenges is demonstrated in the experiment that follows. Four images, namely, Boat, Girl, Girlface, and Pepper are used for the experiment. Additionally, the parameter values are the same as those from the previous experiment. Furthermore, the NHZIS scheme's performance is contrasted with that of the CGD, PCG, SRCME, and T2DFP, where the parameter settings remain as employed in each of the respective papers. In this experiment, the quality of restoration is measured using signal-to-noise ratio (SNR), namely

$$SNR = 20 \times \log_{10}\left(\frac{||\bar{a}||}{||a - \bar{a}||}\right),$$

and peak to signal ratio (PSNR)

$$PSNR = 10 \times \log_{10}\frac{V^2}{MSE},$$

where a represents the original image, $\bar{a}$ represents the de-blurred image, V is maximum absolute value of recovery. We also use MSE and structural similarity index (SSIM), which exhibit the similarity between the actual and recovered images to measure efficiency of the methods. As a general remark, algorithms that yield larger values of SNR, PSNR, and SSIM are regarded as most effective for recovering images much closer to the original ones compared to algorithms with less values of the metrics. Also, algorithms with less value of MSE exhibit better quality of recovery compared to the ones with larger values. It can be observed from the results displayed in Table 6 that NHZIS yields the best of these values in three of the four images considered. In addition to the results in Table 6, Figure 6 displays the original, blurred, and reconstructed images by NHZIS, CGD, PCG, SRCME, and T2DFP, where NHZIS appear to have a slight edge over the other four methods. In order words, Figure 6 shows that the NHZIS method's ability to restore blurry images is marginally

superior to that of CGD, PCG, SRCME, and T2DFP. Consequently, it is evident that the NHZIS method works well for image de-blurring when all factors are taken into account. In the end, these observations imply that, although each technique has advantages, the NHZIS method is clearly a more dependable option for improved image clarity in a wider variety of situations.

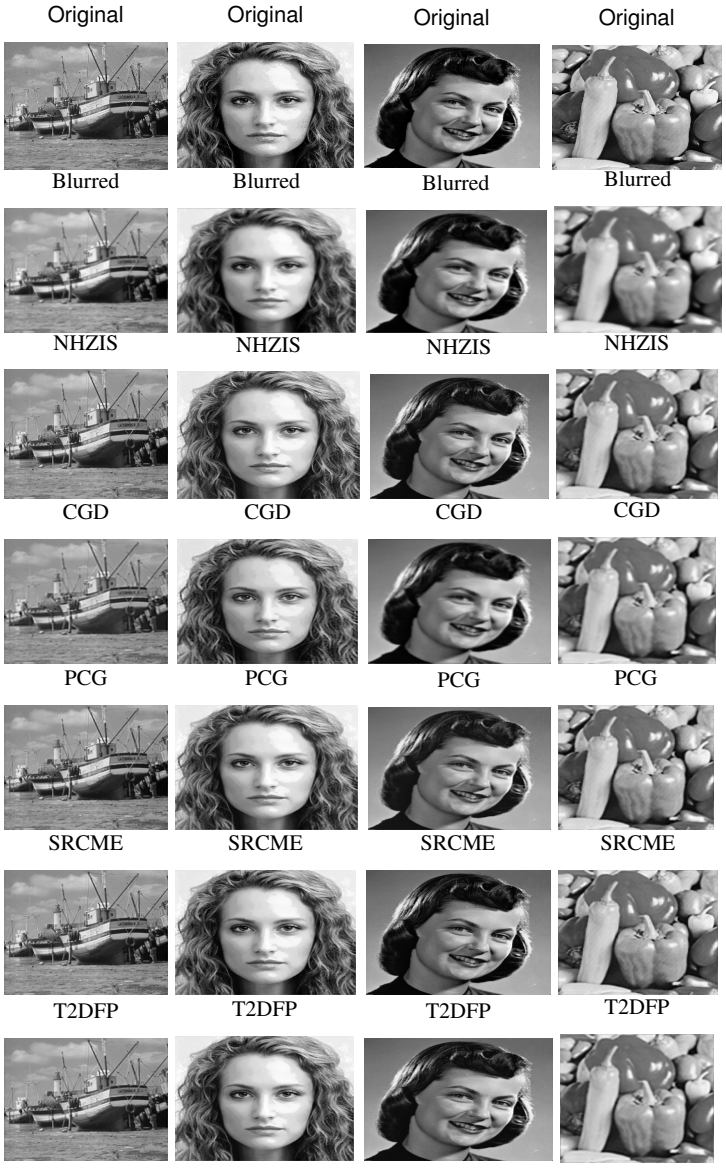

Figure 6. Reconstructed images by the five methods.

7. Concluding remarks

This study explores a variation of the one-parameter HZ method, demonstrating that the parameter θ_k can take values in the interval $(0, \infty)$ while still satisfying the essential criterion for global convergence. By employing the concepts developed by Byrd and Nocedal, we can establish various options for selecting θ_k and propose an alternative HZ-type technique for solving convex constrained nonlinear equations. Due to its derivative-free nature, this innovative approach is well-suited for tackling non-smooth problems. Preliminary numerical experiments comparing four different methods in the literature indicate that the proposed scheme is effective. Additionally, the originality of this method lies in its capacity to decode distorted signals and restore blurry images. The results of the experiments show that this scheme performs competitively and outperforms four other established techniques. As research continues to explore broader applications across various fields, this method could pave the way for advancements that enhance our ability to address complex issues with greater efficiency and accuracy.

Author contributions

Abubakar Sani Halilu: Conceptualization, Methodology, Investigation, Data curation, Writing—original draft preparation; Mohamad A. Mohamed: Validation; Mohammed A. Saleh: Software, Resources, Writing—original draft preparation, Writing—review and editing, Supervision, Funding acquisition; Kabiru Ahmed: Conceptualization, Methodology, Investigation, Data curation, Writing—original draft preparation; Abdulgader Z. Almaymuni: Validation, Formal analysis, Resources, Writing—review and editing, Funding acquisition; Mohammed Y. Waziri: Conceptualization, Validation, Investigation, Writing—review and editing, Supervision; Sulaiman M. Ibrahim: Software, Formal analysis, Data curation, Writing—review and editing, Visualization; Badr Almutairi: Software, Formal analysis, Resources, Visualization, Funding acquisition. All authors have read and agreed to the published version of the manuscript.

Use of Generative-AI tools declaration

The authors declare they have not used Artificial Intelligence (AI) tools in the creation of this article.

Acknowledgments

The Researchers would like to thank the Deanship of Graduate Studies and Scientific Research at Qassim University for financial support (QU-APC-2025).

Conflict of interest

All authors declare no conflicts of interest in this paper.

References

1. S. P. Dirkse, M. C. Ferris, A collection of nonlinear mixed complementarity problems, *Optim. Method. Softw.*, **5** (1995), 319–345. http://doi.org/10.1080/10556789508805619
2. K. Meintjes, A. P. Morgan, A methodology for solving chemical equilibrium systems, *Appl. Math. Comput.*, **22** (1987), 333–361. http://doi.org/10.1016/0096-3003(87)90076-2
3. J. K. Liu, S. J. Li, A projection method for convex constrained monotone nonlinear equations with applications, *Comput. Math. Appl.*, **70** (2015), 2442–2453. http://doi.org/10.1016/0096-3003(87)90076-2
4. Y. Xiao, H. Zhu, A conjugate gradient method to solve convex constrained monotone equations with applications in compressive sensing, *J. Math. Anal. Appl.*, **405** (2013), 310–319. http://doi.org/10.1016/j.jmaa.2013.04.017
5. A. S. Halilu, A. Majumder, M. Y. Waziri, A. M. Awwal, K. Ahmed, On solving double direction methods for convex constrained monotone nonlinear equations with image restoration, *Comput. Appl. Math.*, **40** (2021), 239. http://doi.org/10.1007/s40314-021-01624-1
6. J. Dennis, J. Mor*é*, Quasi-Newton methods, motivation and theory, *SIAM Rev.*, **19** (1977), 46–89. http://doi.org/10.1137/1019005
7. C. Kelly, *Iterative methods for optimization*, Philadelphia: Siam, 1999. http://doi.org/10.1137/1.9781611970920
8. M. V. Solodov, B. F. Svaiter, A globally convergent inexact Newton method for systems of monotone equations, In: *Reformulation: Nonsmooth, Piecewise Smooth, Semismooth and Smoothing Methods*, Boston: Springer, 1998. http://doi.org/10.1007/978-1-4757-6388-1_18
9. W, Cheng, A PRP type method for systems of monotone equations, *Math. Comput. Modell.*, **50** (2009), 15–20. http://doi.org/10.1016/j.mcm.2009.04.007
10. E. Polak, G. Ribi*é*re, Note Sur la convergence de directions conjugèes, *R.I.R.O.*, **3** (1969), 35–43. http://doi.org/10.1051/m2an/196903r100351
11. B. T. Polyak, The conjugate gradient method in extreme problems, *USSR Comput. Math. Math. Phys.*, **9** (1969), 94–112. http://doi.org/10.1016/0041-5553(69)90035-4
12. G. Yu, A derivative-free method for solving large-scale nonlinear systems of equations, *J. Ind. Manag. Optim.*, **6** (2010)149–160. http://doi.org/10.3934/jimo.2010.6.149
13. L. Grippo, F. Lampariello, S. Lucidi, A nonmonotone linesearch technique for Newton's method. *SIAM J. Numer. Anal.*, **23** (1986), 707–716. http://www.jstor.org/stable/2157617
14. D. H. Li, M. Fukushima, A derivative-free linesearch and global convergence of Broyden-like method for nonlinear equations, *Optim. Method. Softw.*, **13** (2000), 583–599.
15. Y. H. Dai, L. Z. Liao, New conjugacy conditions and related nonlinear conjugate gradient methods, *Appl. Math. Optim.*, **43** (2001), 87–101.
16. A. S. Halilu, A. Majumder, M. Y. Waziri, K. Ahmed, A. M. Awwal, Motion control of the two joint planar robotic manipulators through accelerated Dai-Liao method for solving system of nonlinear equatiions, *Eng. Comput.*, **39** (2022), 1802–1840. http://doi.org/10.1108/EC-06-2021-0317

17. X. Z. Jiang, Z. F. Huang, An accelerated relaxed-inertial strategy based CGP algorithm with restart technique for constrained nonlinear pseudo-monotone equations to image de-blurring problems, *J. Comput. Appl. Math.*, **447** (2024), 115887. http://doi.org/10.1016/j.cam.2024.115887

18. M. Y. Waziri, K. Ahmed, A. S. Halilu, Adaptive three-term family of conjugate residual methods for system of monotone nonlinear equations, *Sao Paulo J. Math. Sci.*, **16** (2022), 957–996. http://doi.org/10.1007/s40863-022-00293-0

19. S. B. Salihu, A. S. Halilu, M. Abdullahi, K. Ahmed, P. Mehta, S. Murtala, An improved spectral conjugate gradient projection method for monotone nonlinear equations with application, *J. Appl. Math. Comput.*, **70** (2024), 3879–3915. http://doi.org/10.1007/s12190-024-02121-4

20. J. H. Yin, Q. Huang, J. Jian, D. Han, An inertial-relaxed three-term conjugate gradient projection method for large-scale unconstrained nonlinear pseudo-monotone equations with applications, *J. Comput. Math.*, 2025. http://doi.org/10.4208/jcm.2503-m2024-0175

21. K. Ahmed, M. Y. Waziri, A. S. Halilu, S. Murtala, Descent four-term Dai-Liao type scheme for constrained monotone equations and image de-blurring, *Int. J. Comput. Appl. Math.*, **11** (2025), 223. https://doi.org/10.1007/s40819-025-02039-w

22. W. W. Hager, H. Zhang, A new conjugate gradient method with guaranteed descent and an efficient line search, *SIAM J. Optim.*, **16** (2005), 170–192. http://doi.org/10.1137/030601880

23. W. W. Hager, H. Zhang, A survey of nonlinear conjugate gradient methods, *Pac. J. Optim.*, **2** (2006), 35–58.

24. M. Y. Waziri, K. Ahmed, J. Sabi'u, A family of Hager-Zhang conjugate gradient methods for system of monotone nonlinear equations, *Appl. Math. Comput.*, **361** (2019), 645–660. http://doi.org/10.1016/j.amc.2019.06.012

25. J. Sabi'u, A. Shah, M. Y. Waziri, K. Ahmed, Modified Hager-Zhang conjugate gradient methods via singular value analysis for solving monotone nonlinear equations with convex constraint, *Int. J. Comput. Meth.*, **18** (2020), 04. http://doi.org/10.1142/S0219876220500437

26. M. Y. Waziri, K. Ahmed, A. S. Halilu, J. Sabi'u, Two new Hager-Zhang iterative schemes with improved parameter choices for monotone nonlinear systems and their applications in compressed sensing, *Rairo Oper. Res.*, **56** (2022), 239–273. http://doi.org/10.1051/ro/2021190

27. K. Ahmed, M. Y. Waziri , A. S. Halilu , S. Murtala, Sparse signal reconstruction via Hager-Zhang-type schemes for constrained system of nonlinear equations. *Optimization*, **73** (2023), 1949–1980. http://doi.org/10.1080/02331934.2023.2187255

28. K. Ahmed, M. Y. Waziri, A. S. Halilu, S. Murtala, H. Abdullahi, Signal and image reconstruction with a double parameter Hager-Zhang-type conjugate gradient method for system of nonlinear equations, *Numer. Linear Algebra Appl.*, **32** (2025), e2583. http://doi.org/10.1002/nla.2583

29. C. G. Broyden, The convergence of a class double-rank minimization algorithms, *J. Inst. Math. Appl.*, **6** (1970), 76–90. http://doi.org/10.1093/imamat/6.1.76

30. R. Fletcher, A new approach to variable metric algorithms, *Comput. J.*, **13** (1970), 317–322. http://doi.org/10.1093/comjnl/13.3.317

31. D. Goldfarb, A family of variable metric methods derived by variation mean, *Math. Comput.*, **23** (1970), 23–26. http://doi.org/10.2307/2004873

32. D. F. Shanno, Conditioning of quasi-Newton methods for function minimization, *Math. Comput.*, **24** (1970), 647–656. http://doi.org/10.2307/2004840

33. A. Liao, Modifying BFGS method, *Oper. Res. Lett.*, **20** (1997), 171–177. http://doi.org/10.1016/S0167-6377(96)00050-8

34. N. Andrei, A double parameter scaled BFGS method for unconstrained optimization, *J. Comput. Appl. Math.*, **332** (2018), 26–44. http://doi.org/10.1016/j.cam.2017.10.009

35. S. Babaie-Kafaki, Z. Aminifard, Two parameter scaled memoryless BFGS methods with a nonmonotone choice for the initial step length, *Numer. Algor.*, **82** (2019), 1345–1357. http://doi.org/10.1007/s11075-019-00658-1

36. N. Andrei, A double-parameter scaling Broyden–Fletcher–Goldfarb–Shanno method based on minimizing the measure function of Byrd and Nocedal for Unconstrained Optimization, *J. Optim. Theory Appl.*, **178** (2018), 191–218. http://doi.org/10.1007/s10957-018-1288-3

37. R. Byrd, J. Nocedal, A tool for the analysis of quasi-Newton methods with application to unconstrained minimization, *SIAM J. Numer. Anal.*, **26** (1989), 727–739. http://doi.org/10.1137/0726042

38. S. Babai-Kafaki, On the sufficient descent condition of the Hager-Zhang conjugate gradient methods, *40R-Q. J. Oper. Res.*, **12** (2014), 285–292. http://doi.org/10.1007/s10288-014-0255-6

39. J. Sabi'u, A. Shah, M. Y. Waziri, Two optimal Hager-Zhang conjugate gradient methods for solving monotone nonlinear equations, *Appl. Numer. Math.*, **153** (2020), 217–233. http://doi.org/10.1016/j.apnum.2020.02.017

40. J. Sabi'u, A. Shah, M. Y. Waziri, A modified Hager-Zhang conjugate gradient method with optimal choices for solving monotone nonlinear equations, *Int. J. Comput. Math.*, **99** (2021), 332–352. http://doi.org/10.1080/00207160.2021.1910814

41. R. H. Byrd, J. Nocedal, A tool for the analysis of quasi-Newton methods with application to unconstrained minimization, *SIAM J. Numer. Anal.*, **26** (1989), 727–739. http://doi.org/10.1137/0726042

42. P. Gao, W. Zheng, T. Wang, Y. Li, F. Li, Signal recovery with constrained monotone nonlinear equations, *J. Appl. Anal. Comput.*, **13** (2023), 2006–2025. http://doi.org/10.11948/20220335

43. L. Pengjie, A three-term derivative-free projection method with BFGS-like update and its accelerated variant, *Optimization*, 2025, 1–35. http://doi.org/10.1080/02331934.2025.2526727

44. W. La Cruz, A Spectral algorithm for large-scale systems of nonlinear monotone equations, *Numer. Algor.*, **76** (2017), 1109–1130. http://doi.org/10.1007/s11075-017-0299-8

45. E. D. Dolan, J. J. Moré, Benchmarking optimization software with performance profiles, *Math. Program.*, **91** (2002), 201–213. http://doi.org/10.1007/s101070100263

46. M. R. Banham, A. K. Katsaggelos, Digital image restoration, *IEEE Signal Process, Mag.*, **14** (1997), 24–41. http://doi.org/10.1109/79.581363

47. C. L. Chan, A. K. Katsaggelos, A. V. Sahakian, Image sequence filtering in quantum-limited noise with applications to low-dose fluoroscopy, *IEEE Trans. Med. Imaging*, **12** (1993), 610–621. http://doi.org/10.1109/42.241890

48. C. H. Slump, Real-time image restoration in diagnostic X-ray imaging, the effects on quantum noise, *11th IAPR International Conference on Pattern Recognition*, 1992, 693–696. http://doi.org/10.1109/ICPR.1992.201871

49. T. Elaine, Y. Wotao, Z. Yin, A fixed-point continuation method for ℓ_1-regularized minimization with applications to compressed sensing, *SIAM J. Optim.*, **19** (2008), 1107–1130. http://doi.org/10.1137/070698920

50. J. S. Pang, Inexact Newton methods for the nonlinear complementarity problem, *Math. Program.*, **36** (1986), 54–71. http://doi.org/10.1007/BF02591989

51. A. T. Mario, R. Figueiredo, D. Nowak, An EM algorithm for wavelet-based image restoration, *IEEE Trans. Image Process.*, **12** (2003), 906–916. http://doi.org/10.1109/TIP.2003.814255

52. M. Figueiredo, R. Nowak, S. J. Wright, Gradient projection for sparse reconstruction, application to compressed sensing and other inverse problems, *IEEE J-STSP*, **1** (2007), 586–597. http://doi.org/10.1109/JSTSP.2007.910281

53. Y. Xiao, Q. Wang, Q. Hu, Non-smooth equations based method for ℓ_1 – *norm* problems with applications to compressed sensing, *Nonlinear Anal. Theory Methods Appl.*, **74** (2011), 3570–3577. http://doi.org/10.1016/j.na.2011.02.040

AIMS Press